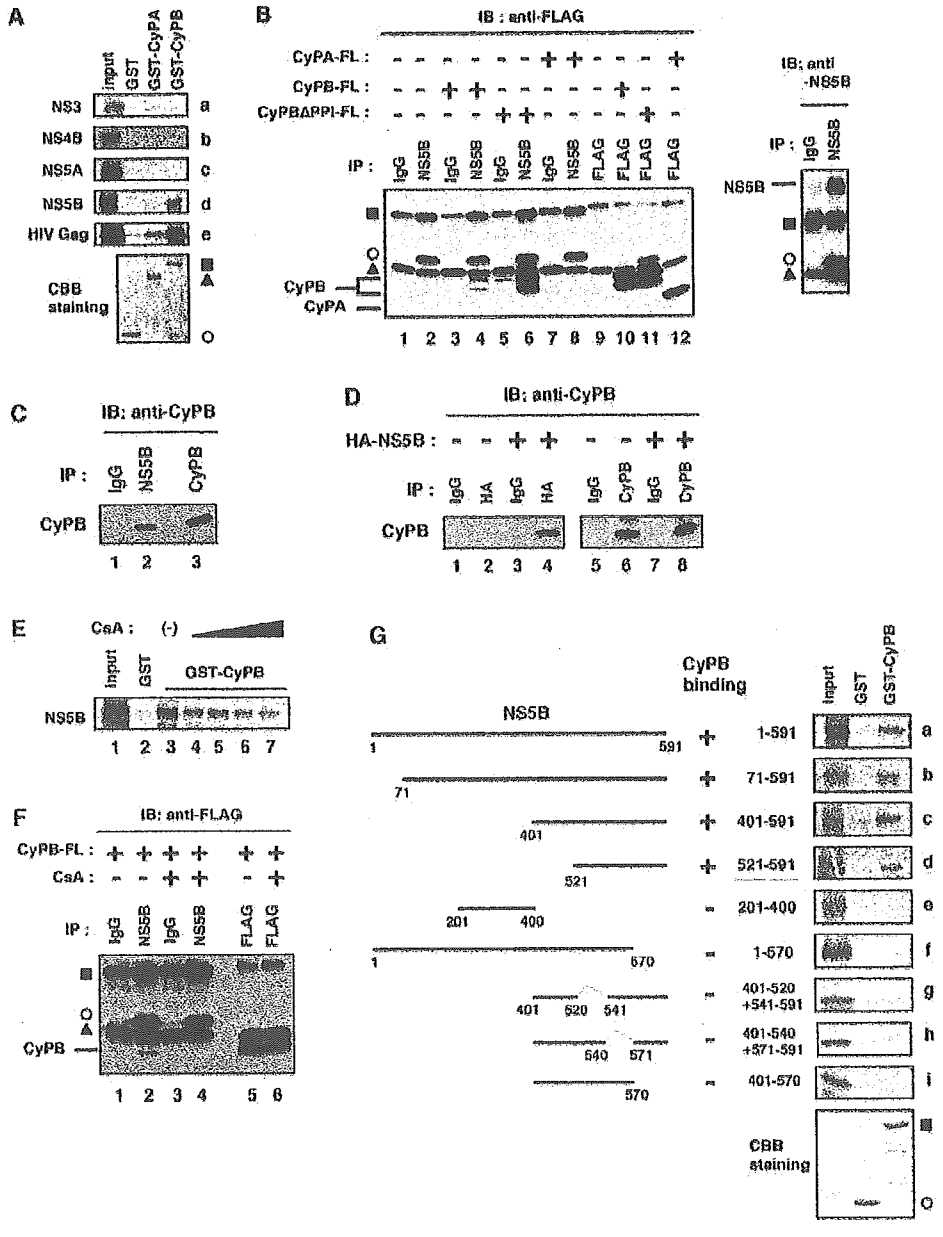

Figure 3. CyPB Interacted with HCV NS5B

(A) [^{35}S]-labeled in vitro translation products of HCV NS3 (panel a), NS4B (panel b), NS5A (panel c), NS5B (panel d), and HIV-1 Gag as a positive control (panel e) were incubated with recombinant GST fusions of CyPA or CyPB (GST-CyPA or GST-CyPB, respectively) or with GST as a negative control. "Input" designated the signal for 1/10 of the amount of [^{35}S]-labeled product used in the pull-down assay. CBB staining patterns for the pulled-down proteins are shown in the bottom panel. Open circle, GST; closed triangle, GST-CyPA; and closed square, GST-CyPB.

(B) Coimmunoprecipitation from lysates of MH-14 cells transfected with expression plasmids for FLAG-tagged CyPA (CyPA-FL) (lanes 7, 8, and 12), CyPB (CyPB-FL) (lanes 3, 4, and 10), CyPBΔPPI (CyPBΔPPI-FL) (lanes 5, 6, and 11), or empty vector (lanes 1, 2, and 9 and right panel). The plasmids used for transfection are indicated at the top of the panel by + or –. "IP" designates the antibodies used for immunoprecipitation. Coimmunoprecipitated proteins were detected by immunoblot analysis using either anti-FLAG (left) or anti-NS5B (right) antibodies, respectively. Closed square, Ig heavy chain; closed triangle, Ig light chain; and open circle, nonspecific band. CyPA, CyPB or CyPBΔPPI, and NS5B are indicated. Ectopically expressed CyPB showed a double band, consistent with the previous report (Price et al., 1994). The upper-slight band of CyPBΔPPI in lane 5 is likely to show nonspecific binding, because it was not precipitated with IgG in a buffer containing higher concentration of NP-40 (1% NP-40) (data not shown).

(C) Coimmunoprecipitation of endogenous CyPB with NS5B in MH-14 cells. The data are presented as in (B). The immunoprecipitates were detected with an anti-CyPB antibody.

(D) Coimmunoprecipitation of endogenous CyPB with exogenous NS5B in Huh-7 cells. Huh-7 cells were transfected with an expression

protein-protein interactions, nuclear import, enzymatic activity, or protein phosphorylation. In this study, we demonstrated that CyPB also modulated the activity of RNA-protein binding. This information will significantly impact our understanding of the molecular functions of CyP.

Regarding the role of CyP in virus proliferation, CyPA has been reported to be involved in the life cycle of HIV-1. CyPA binds HIV-1 Gag (Luban et al., 1993) and is incorporated into viral particles (Franke et al., 1994; Thali et al., 1994). This CyPA promotes viral infectivity (Braaten and Luban, 2001; Towers et al., 2003). HIV-1 Gag, however, binds to not only CyPA but also most other members of the CyP family (Braaten and Luban, 2001; Luban et al., 1993). In contrast to HIV-1 Gag, HCV NS5B bound CyPB, but not CyPA. Among the CyP family members examined, only CyPB regulated HCV genome replication. The subcellular localization of each CyP subtype varies; CyPA is found in the cytoplasm and nucleus, CyPD in the mitochondria, and CyPE in the nucleus (Takahashi, 1999). CyPB is located mainly in the lumen of the ER (Price et al., 1994; Takahashi, 1999). A subset of CyPB, however, was speculated to localize in the cytoplasm or in ER substructures on the cytoplasmic side (Bram et al., 1993). We found that a portion of CyPB localized on the cytoplasmic face of the ER irrespective of the presence of HCV replicon (Figure 4B), consistent with this previous speculation.

Almost all HCV proteins and genomic RNA are located around the ER (Bartenschlager and Lohmann, 2001). The majority of events in the HCV life cycle, including genome replication, protein maturation, assembly, and budding, occur around intracellular ER-like membranes (Bartenschlager and Lohmann, 2001). NS5B mainly localizes on the cytoplasmic side of the ER membrane through its C-terminal 571–591 aa hydrophobic region (Schmidt-Mende et al., 2001). A subset of the total NS5B participates in the RC, which is thought to have a cytoplasmic side membrane topology and is surrounded by a membrane structure (Aizaki et al., 2004). We cannot conclude clearly where CyPB-NS5B-RNA association occurs. The 521–591 aa region of NS5B, which is the binding region for CyPB, however, is thought to be inserted in the ER lipid bilayer membrane on the cytoplasmic face (Schmidt-Mende et al., 2001). A part of CyPB was also found on the cytoplasmic face of the membranes as described above. Moreover, crosslinking analysis (Figure 4C) suggests the interaction of CyPB with the HCV RNA-NS5B complex, which is likely to occur mainly in the RC. Thus, CyPB likely interacts with NS5B on the cytoplasmic face within the RC compartment (and in the lipid bilayer membrane).

Viral polymerases are promising targets for the development of antiviral agents. Several chemicals targeting NS5B have anti-HCV activity (Wu and Hong, 2003). These compounds directly inhibit the activity of recombinant NS5B in vitro. In addition to these typical anti-HCV compounds, inhibition of the association of CyPB with NS5B may serve as a strategy for the design of antiviral therapeutics. Our findings not only reveal one of the mechanisms of viral replication in the cells but also may lead to the development of antiviral therapeutics.

Experimental Procedures

Cell Culture and Transfection

Huh-7 and cured MH-14 cells (Murata et al., 2005) were cultured in Dulbecco's modified Eagle medium (DMEM) (Invitrogen) supplemented with 10% fetal bovine serum, L-glutanime (Invitrogen), MEM nonessential amino acids (Invitrogen), and kanamycin (Meiji). MH-14 cells, carrying HCV subgenomic replicon (Miyanari et al., 2003), were cultured in the same medium supplemented with 300 μg/ml G418 (Invitrogen). Plasmid transfection was performed as described previously (Watashi et al., 2003b). RNA transfection for the reporter assay was achieved by using DMrie-C transfection reagent (Invitrogen) as recommended by the manufacturer. siRNA was transfected by using siLentFect (BIORAD) according to the manufacturer's protocol.

Reagents

CsA was purchased from Sigma. The CsA derivatives 8′-OH-MeBmt^{1}-Cs, MeAla^{6}-Cs, D-lys^{8}-Cs, MeVal^{4}-Cs, cyclosporin H, NIM811, and PSC833 and the macrolide type CyP inhibitors sanglifehrin A and B were kindly provided by Novartis (Basel, Switzerland). The characteristic feature of each CsA derivative is shown in Figure 1A (for details, see Billich et al. [1995], Loor et al. [2002], and Silverman et al. [1997]). (D-lys^{8})Cs binds CyP in vitro. In cells, however, the effective binding affinity to CyP is low because of inefficient cellular uptake (Billich et al., 1995).

Immunoblot Analysis

Immunoblot analysis was performed essentially as described previously (Watashi et al., 2003b).

Antibodies

The antibodies used in this experiment were anti-NS5A (a generous gift from Dr. Takamizawa, Osaka University), anti-NS5B (10 and 14; kindly provided by Dr. Kohara, Tokyo Metropolitan Institute of Medical Science), anti-actin (Sigma), anti-CyPA (Upstate Cell Signaling), anti-CyPB (Affinity BioReagents), anti-FLAG (M2; Sigma), anti-HA (3F10; Roche), anti-BrdU (Sigma), anti-IκBα (Santa Cruz), anti-PDI (StressGen), and anti-calnexin (StressGen) antibodies.

Real-Time RT-PCR Analysis

Real-time RT-PCR analysis was performed as described previously (Watashi et al., 2003a).

RNAi Technique

siRNA duplexes (si-CyPA, 5′-AAGCATACGGGTCCTGGCATC-3′; si-CyPB, 5′-AAGGTGGAGAGCACCAAGACA-3′; and si-CyP(broad), 5′-AAGCATGTGGTGTTTGGCAAA-3″) containing 3′dTdT over-

plasmid for HA-tagged NS5B (lanes 3, 4, 7, and 8) or an empty vector (lanes 1, 2, 5, and 6). The immunoprecipitates were detected by an anti-CyPB antibody.

(E and F) The interaction of CyPB with NS5B was disrupted by CsA treatment. In (E), a GST pull-down assay between GST-CyPB and NS5B was performed in the absence (lane 3) or presence (lanes 4–7) of CsA. The concentrations of CsA in lanes 4–7 are 0.8, 4, 8, and 16 μg/ml, respectively. In (F), coimmunoprecipitation between CyPB-FL and NS5B in MH-14 cells treated without (lanes 1, 2, and 5) or with 3 μg/ml CsA (lanes 3, 4, and 6) was analyzed.

(G) Mapping of the regions of NS5B responsible for the interaction with CyPB. At the left of the panel, schematic representation of the full-length and truncated mutants of NS5B is shown. The numbers indicate the amino acids residue numbers in NS5B. "CyPB binding" summarizes the results of a GST pull-down assay by ±; GST pull-down data are presented as described in (A).

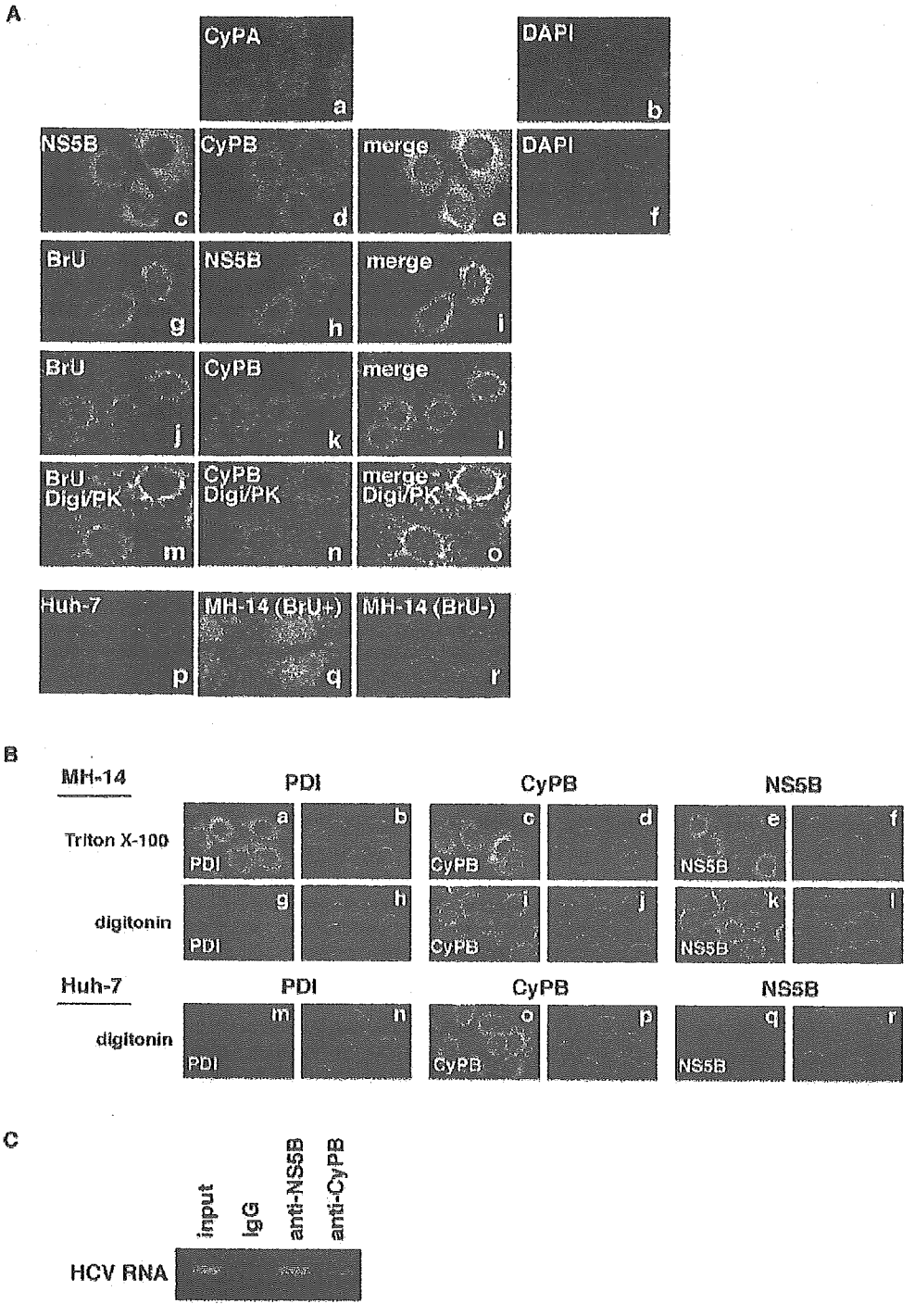

Figure 4. Colocalization of CyPB with NS5B around the Endoplasmic Reticulum

(A) CyPB colocalized with NS5B. Indirect immunofluorescence analysis was performed on MH-14 cells incubated in the absence (panels a–f and r) or presence of actinomycin D/BrU (panels g–o and q). Huh-7 cells were treated with actinomycin D/BrU as a negative control (panel p). Prior to immunofluorescence analysis with permeabilization by Triton X-100, cells were treated with digitonin (Digi) followed by digestion with 0.3 μg/ml proteinase K (PK) in panels m–o. The primary antibodies used were anti-CyPA (panel a, red), anti-CyPB (panels d, k, and n, red), anti-NS5B (panel c, green and panel h, red), and anti-BrdU (panels g, j, m, and p–r, green) antibodies. DAPI was used to visualize the nuclei (panels b, f, and p–r, blue). Panels a–b, c–f, g–i, j–l, and m–o show the same cells. Merged images of green and red signals are shown in panels e, i, l, and o. Panels p–r are the merged images of green (BrU) and blue (DAPI) signals.

(B) A portion of CyPB was located on the cytoplasmic face of the intracellular membrane. MH-14 cells were fixed and followed by permeabili-

hanging sequences were synthesized (QIAGEN). A control nucleotide, si-control, was purchased from Dharmacon (nonspecific control duplex IX). si-CyPC, si-CyPE, and si-CyPH were obtained from Ambion (predesigned siRNA). The sequence of si-CyP(broad) matches 100% with CyPA and CyPB mRNAs, a 20 bp match with CyPH, a 19 bp match with CyPC and CyP40, and a 17 bp match with CyP33. The sequence of si-CyPA and si-CyPB does not have significant identity to mRNA for CyPB and CyPA, respectively.

RT-PCR Analysis

RT-PCR analysis was performed as described (Watashi et al., 2003b) by using the following primer sets: 5′-GTTGGATCCATG GGCCCGGGTC-3′ and 5′-GTTCTCGAGTCACCAATCAGCGATC-3′ for the detection of CyPC, 5′-GTTGAATTCATGGCCACCACCAAG-3′ and 5′-GTTCTCGAGTCACACGTACTCCCCAC-3′ for CyPE, and 5′-GTTGGATCCATGGCGGTGGCAAATTC-3′ and 5′-GTTCTCGAG CTACATCTCCCCACAC-3′ for CyPH.

Luciferase Assay

A luciferase assay monitoring HCV replication levels was performed as previously described (Murata et al., 2005). The reporter RNAs used in this study were LMH14, LMH14(GHD), in which the GDD polymerase motif of NS5B was replaced by GHD to lose replication activity, and LMH14(P540A), in which the proline at position 540 of NS5B was replaced by alanine.

Plasmid Constructs

The CyPA and CyPB cDNAs were obtained by RT-PCR from a human liver cDNA library (Clontech) template by using the following primers: 5′-GTTGGATCCGCCATGGTCAACCCCACCG-3′ and 5′-GTT GAATTCTTCGAGTTGTCCACAGTC-3′ for CyPA and 5′-GTTGGA TCCGCCATGCTGCGCCTCTCC-3′ and 5′-GTTGAATTCCTCCTTG GCGATGGCAA-3′ for CyPB. pGEX-CyPA and pGEX-CyPB, which encode glutathione S-transferase (GST) fusions of CyPA and CyPB were constructed by insertion of the BamHI-EcoRI fragments into the appropriate site of the pGEX-6P1 vector (Clontech). The pCMV-CyPA-FL and pCMV-CyPB-FL plasmids expressing FLAG-tagged CyPA and CyPB, respectively, were obtained by inserting the CyPA and CyPB fragments into the BamHI-EcoRI site of the pCMV-FLAG(C) vector. CyPBΔPPI, of which arginine and phenylalanine at position 95 and 100 of CyPB were replaced by alanines, was an enzymatic-inactive mutant of CyPB (Rycyzyn and Clevenger, 2002). The subcloning of pCMV-CyPBΔPPI-FL, which encodes a FLAG-tagged CyPBΔPPI, was performed essentially as described (Rycyzyn and Clevenger, 2002). Expression plasmids for HCV NS3, NS4B, NS5A, and NS5B (pcDNA-NS3, pcDNA-NS4B, pcDNA-NS5A, and pcDNA-NS5B, respectively) were generated by insertion of PCR-amplified fragments encoding each HCV protein into the pcDNA3 vector (Invitrogen). The series of plasmids expressing deletion mutants of NS5B were constructed by inserting into the pcDNA3 vector various fragments amplified by PCR using appropriate synthetic oligonucleotides as primers and pLMH14 as a template. The primers for oligonucleotide-directed mutagenesis used to generate the NS5B(P540A) mutant were 5′-ACTCCAATTGCGG CTGCGTCC-3′ and 5′-GGACGCAGCCGCAATTGGAGT-3′. LMH14 and LMH14(GHD) have been described previously (Murata et al., 2005). The expression plasmid for HIV-1 Gag was kindly provided by Dr. Adachi, Institute of Health Biosciences, The University of Tokushima.

GST Pull-Down Assay

A GST pull-down assay was performed as described previously (Watashi et al., 2003b).

Immunoprecipitation Assay and RNA-Protein Binding Precipitation Assay

An immunoprecipitation assay was essentially performed as described (Watashi et al., 2003b). For the RNA-protein binding precipitation assay, either cells or digitonin/protease-treated cells were lysed in IP buffer containing 50 mM Tris-HCl (pH 8.0), 150 mM NaCl, 0.5% NP-40, and 1 mM PMSF. After centrifugation, supernatants were incubated for 2 hr with poly-U or protein G Sepharose resin as a negative control (Amersham Biosciences). After four washes with IP buffer, precipitates were analyzed by immunoblot analysis.

Indirect Immunofluorescence Analysis

The normal indirect immunofluorescence analysis in Figures 4A and 4B, panels a–f, was performed as described previously (Watashi et al., 2003b). Briefly, the cells were fixed, and permeabilization with 0.1% Triton X-100 followed. These cells were subjected to the antibody reaction to detect each protein. In Figure 4A, panels g–r, de novo-synthesized HCV RNA was labeled with 5-BrU. Cells were treated with 10 μg/ml actinomycin D to block RNA transcription by cellular DNA-dependent RNA polymerases (Restrepo-Hartwig and Ahlquist, 1996). After a 30 min incubation, 40 mM BrU was added to the culture medium for labeling RNA (Fuchsova et al., 2002). After an additional 2 hr, the cells were subjected to immunofluorescence analysis. In the modified immunofluorescence analysis (Watashi et al., 2001) in Figure 4B, panels g–r, we treated the cells with 50 μg/ml digitonin at 27°C for 5 min to permeabilize the plasma membrane, but not the intracellular membrane. After washing out the cytosol, these cells were fixed and subjected to the antibody reaction.

Crosslinking Assay for the Detection of RNA-Protein Complex

Crosslinking and the subsequent immunoprecipitation were essentially performed as described (Watashi et al., 2003b). The immunoprecipitation was done in the presence of RNase inhibitor and polydI-dC. Recovered immunocomplexes were digested with proteinase K and treated with phenol/chloroform. RT-PCR was performed with the extracted RNA and 5′-TCCCGGTTGGACTTGTCC-3′ and 5′-GCCTATTGGCCTGGAGTG-3′ as a template and primer sets, respectively, by using a one-step RNA PCR kit.

Cell Permeabilization with Digitonin Followed by Digestion with Protease

Digitonin/protease treatment was performed as described previously (Miyanari et al., 2003). Briefly, cells were permeabilized by a 5 min incubation in buffer B containing 50 μg/ml digitonin at 27°C. After two washes in buffer B, cells were treated for 5 min with varying concentrations of proteinase K at 37°C.

RNA Synthesis with the Replication Complex

RNA synthesis reaction was performed as described (Miyanari et al., 2003), using reaction times of 0.5, 1, 2, 4, 6, 12, and 24 hr.

In Vitro RNA Binding Assay

An in vitro RNA binding assay was performed by using poly-U or poly-A Sepharose as a model RNA substrate, as described previously (Ishii et al., 1999). In vitro-translated [^{35}S]-labeled products and poly-U, poly-A, or protein G Sepharose resin as a negative

---

zation with 0.1% Triton X-100 to detect PDI (panel a), CyPB (panel c), and NS5B (panel e) by normal immunofluorescence analysis as a control experiment (Triton X-100). In panels g–r (digitonin), MH-14 (panels g–l) and Huh-7 cells (panels m–r) were permeabilized with 50 μg/ml digitonin followed by extensive washes. These cells were then fixed and subjected to detection of PDI (panels g and m), CyPB (panels i and o), and NS5B (panels k and q). DAPI (panels b, d, f, h, j, l, n, p, and r) shows the nuclear staining in the same cells as that shown in panels a, c, e, g, i, k, m, o, and q.

(C) CyPB associated with HCV RNA-NS5B complex in the cells. Formaldehyde-crosslinked RNA-protein complexes in MH-14 cells were immunoprecipitated with anti-NS5B, anti-CyPB, or normal rabbit IgG (IgG). The RNA extracted from the immunoprecipitates was amplified by RT-PCR as described in the Experimental Procedures. "Input" designated the signal for 1/50 of the amount of cell lysate used in the immunoprecipitation assay.

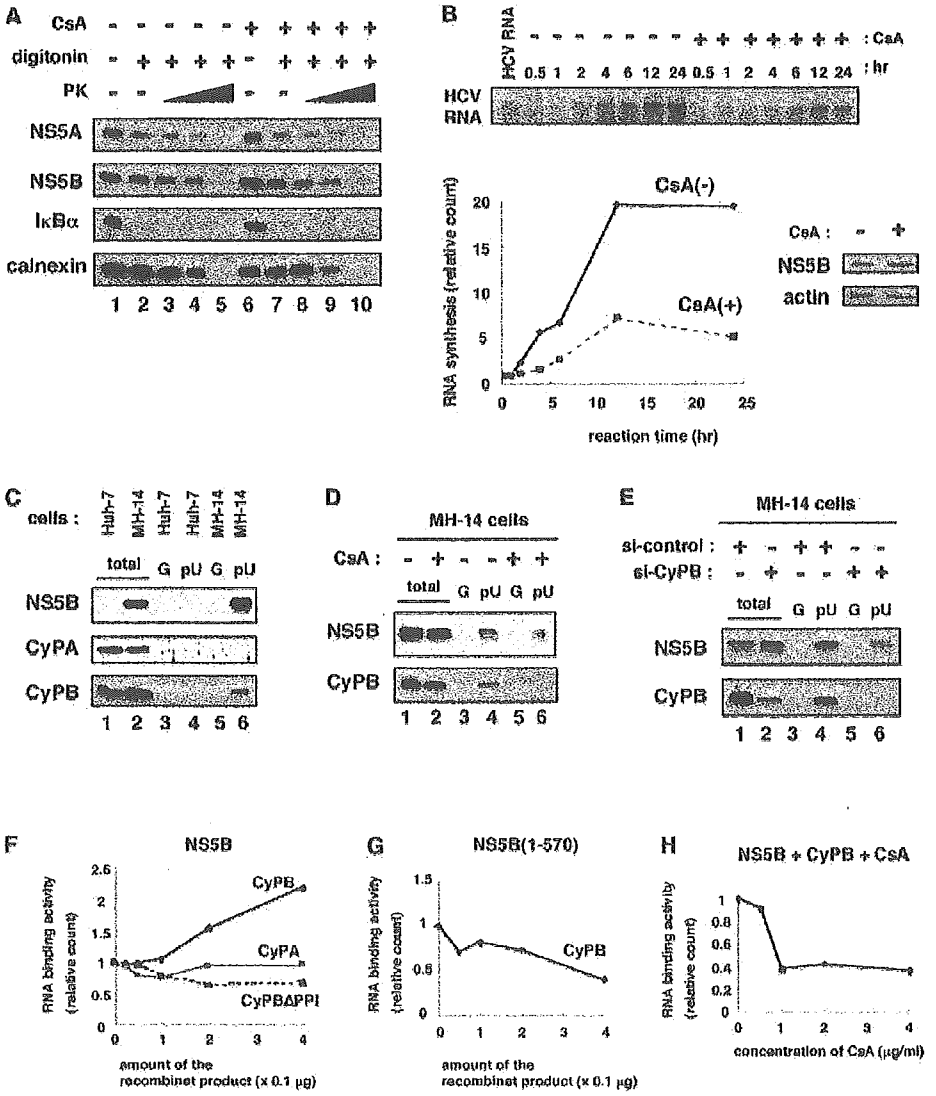

Figure 5. CyPB Stimulated RNA Binding Activity of NS5B

(A) Quantitation of the amount of HCV proteins in the digitonin/protease-resistant fraction. MH-14 cells were treated without (lanes 1–5) or with (lanes 6–10) 3 μg/ml CsA for 24 hr. Cells were then treated without (lanes 1 and 6) or with 50 μg/ml digitonin, followed by digestion with varying concentrations of PK (0 μg/ml for lanes 1, 2, 6, and 7, 0.03 μg/ml for lanes 3 and 8, 0.1 μg/ml for lanes 4 and 9, and 0.3 μg/ml for lanes 5 and 10). NS5A, NS5B, IκBα, and calnexin in whole-cell lysate were detected by immunoblot analysis.

(B) RNA synthesis activity in the HCV RC. MH-14 cells were treated without or with 3 μg/ml CsA for 24 hr. After isolating the RC by digitonin permeabilization, RNA synthesis reaction was performed with varying reaction times (0.5, 1, 2, 4, 6, 12, and 24 hr). At the top of the panel, treatment of CsA and reaction time is summarized. "HCV RNA" indicates the in vitro-synthesized HCV subgenomic replicon RNA. In the lower left panel, the radioactivity of synthesized RNA is plotted against the reaction time. The lower right panels show the protein expression levels of NS5B and actin.

(C) An RNA-protein binding precipitation assay was performed by using Huh-7 or MH-14 cells as described in the Experimental Procedures. The resultant precipitates were detected by immunoblot analysis with anti-NS5B (top), anti-CyPA (middle), and anti-CyPB (bottom) antibodies. "Total" indicates 1/6 of the amount of cell lysate used in the precipitation assay. "G" and "pU" designate the samples using protein G Sepharose and poly-U Sepharose as a resin, respectively.

(D) MH-14 cells treated with digitonin followed by digestion in 0.5 μg/ml PK were used for an RNA-protein binding precipitation assay with anti-NS5B antibody (top). Prior to the assay, CsA was treated (lanes 2, 5, and 6) or left untreated (lanes 1, 3, and 4) for 24 hr. CyPB levels were also examined in CsA-treated or untreated cells (bottom).

(E) MH-14 cells were transfected with si-control or si-CyPB. After 72 hr, cells were treated with digitonin/PK and analyzed as in (C).

(F–H) An in vitro binding assay was performed as described in the Experimental Procedures. [^{35}S]-labeled in vitro translation products of either the full-length NS5B (F and H) or the 1–570 aa region of NS5B (G) were incubated with poly-U Sepharose in the presence of either recombinant GST-CyPB (F–H), GST-CyPA (F), or GST-CyPBΔPPI (F). In (H), varying concentrations of CsA were also added to the reaction mixtures. The radioactivity of NS5B protein in the pulled-down fraction was counted to plot against either the amount of the recombinant product (F and G) or the concentration of CsA (H). In (F), the solid line represents being in the presence of GST-CyPB; the broken line, GST-CyPBΔPPI; and the faint line, GST-CyPA. These results were reproduced in three independent experiments.

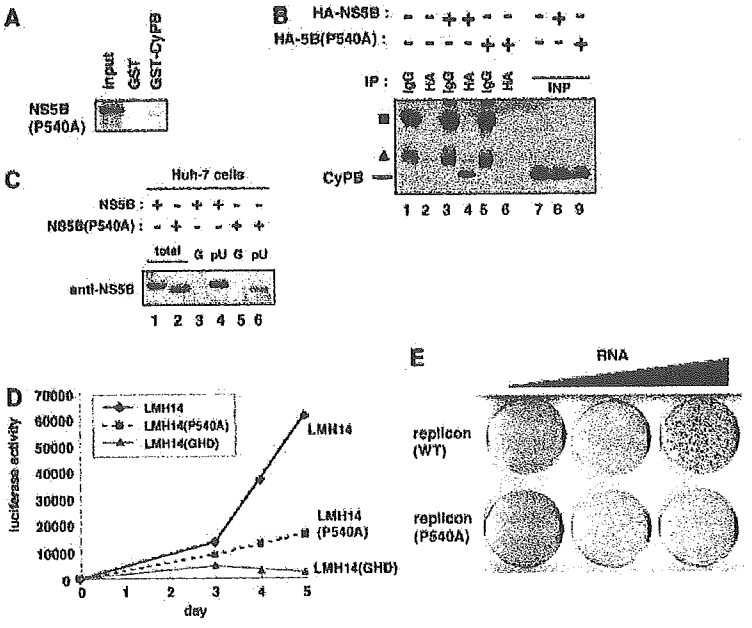

Figure 6. Association of CyPB with NS5B Was Critical for the Efficient Replication of the HCV Genome

(A) A GST pull-down assay was performed and presented as described in Figure 3A.

(B) An immunoprecipitation assay was performed as described in Figure 3B. The expression plasmid for HA-tagged NS5B (lanes 3, 4, and 8) and NS5B(P540A) (lanes 5, 6, and 9) and empty vector (lanes 1, 2, and 7) was used for the transfection. "INP" indicates 1/6 of the amount of cell lysate used for the immunoprecipitation.

(C) An RNA-protein binding precipitation assay was performed by using Huh-7 cells transfected with the expression vector for NS5B (lanes 1, 3, and 4) or NS5B(P540A) (lanes 2, 5, and 6) as described in Figure 5C.

(D) Luciferase assays were performed and are presented as in Figure 2F. Solid line, LMH14; broken line, LMH14(P540A); and faint line, LMH14(GHD).

(E) Colony formation assay. The subgenomic replicon RNA (replicon[wt]) and a replicon RNA carrying the P540A mutation in NS5B (replicon[P540A]) at various amount (2.5 μg in the left wells, 5 μg in the center wells, and 10 μg in the right wells) was transfected into Huh-7 cells. The colony formation assay was performed as described in the Experimental Procedures.

control were incubated in the presence of a varying amount of GST-fusion proteins, including GST-CyPB, GST-CyPA, and GST-CyPBΔPPI, at 4°C for 1–12 hr. In Figure 5H, CsA was added simultaneously. After five washes, resin bound radiolabeled proteins were fractionated, and its radioactivity was quantitated.

Colony Formation Assay

Plasmids were linearized with XbaI and transcribed into RNA in vitro by using a MEGAscript T7 kit (Ambion) according to the manufacturer's protocol. In vitro-transcribed RNA (2.5–10 μg) was transfected into Huh-7 cells by using DMrie-C transfection reagent. At 48 hr posttransfection, 1 mg/ml G418 was added to the medium. ~3 weeks later, cells were fixed and stained with crystal violet.

Acknowledgments

We are grateful to Dr. Takamizawa at Osaka University for an anti-NS5A antibody, Dr. Kohara at Tokyo Metropolitan Institute of Medical Science for an anti-NS5B antibody, and Dr. Adachi at the Institute of Health Biosciences, the University of Tokushima for an expression plasmid for HIV-1 Gag. We also appreciate Novartis (Basel, Switzerland) for providing CsA derivatives and sanglifehrins. This work was supported by grants in aid for cancer research and for the second-term comprehensive 10 year strategy for cancer control from the Ministry of Health, Labor, and Welfare; through grants in aid for scientific research from the Ministry of Education, Culture, Sports, Science and Technology; by grants in aid for Research for the Future from the Japanese Society for the Promotion of Science; and by the Program for Promotion of Fundamental Studies in Health Science of the Organization for Pharmaceutical Safety and Research (OPSR) of Japan.

Received: February 9, 2005
Revised: April 13, 2005
Accepted: May 18, 2005
Published: June 30, 2005

References

Aizaki, H., Lee, K.J., Sung, V.M., Ishiko, H., and Lai, M.M. (2004). Characterization of the hepatitis C virus RNA replication complex associated with lipid rafts. Virology *324*, 450–461.

Bartenschlager, R., and Lohmann, V. (2001). Novel cell culture systems for the hepatitis C virus. Antiviral Res. *52*, 1–17.

Billich, A., Hammerschmid, F., Peichl, P., Wenger, R., Zenke, G., Quesniaux, V., and Rosenwirth, B. (1995). Mode of action of SDZ NIM *811*, a nonimmunosuppressive cyclosporin A analog with activity against human immunodeficiency virus (HIV) type 1: interference with HIV protein-cyclophilin A interactions. J. Virol. *69*, 2451–2461.

Braaten, D., and Luban, J. (2001). Cyclophilin A regulates HIV-1 infectivity, as demonstrated by gene targeting in human T cells. EMBO J. *20*, 1300–1309.

Bram, R.J., Hung, D.T., Martin, P.K., Schreiber, S.L., and Crabtree, G.R. (1993). Identification of the immunophilins capable of mediating inhibition of signal transduction by cyclosporin A and FK506: roles of calcineurin binding and cellular location. Mol. Cell. Biol. *13*, 4760–4769.

Brazin, K.N., Mallis, R.J., Fulton, D.B., and Andreotti, A.H. (2002). Regulation of the tyrosine kinase Itk by the peptidyl-prolyl isomerase cyclophilin A. Proc. Natl. Acad. Sci. USA *99*, 1899–1904.

Colgan, J., Asmal, M., Neagu, M., Yu, B., Schneidkraut, J., Lee, Y., Sokolskaja, E., Andreotti, A., and Luban, J. (2004). Cyclophilin A regulates TCR signal strength in CD4+ T cells via a proline-directed conformational switch in Itk. Immunity *21*, 189–201.

Duina, A.A., Chang, H.C., Marsh, J.A., Lindquist, S., and Gaber, R.F. (1996). A cyclophilin function in Hsp90-dependent signal transduction. Science *274*, 1713–1715.

Egger, D., Wolk, B., Gosert, R., Bianchi, L., Blum, H.E., Moradpour, D., and Bienz, K. (2002). Expression of hepatitis C virus proteins induces distinct membrane alterations including a candidate viral replication complex. J. Virol. *76*, 5974–5984.

El-Hage, N., and Luo, G. (2003). Replication of hepatitis C virus RNA occurs in a membrane-bound replication complex containing nonstructural viral proteins and RNA. J. Gen. Virol. *84*, 2761–2769.

Fischer, G., Tradler, T., and Zarnt, T. (1998). The mode of action of peptidyl prolyl cis/trans isomerases in vivo: binding vs. catalysis. FEBS Lett. *426*, 17–20.

Franke, E.K., Yuan, H.E., and Luban, J. (1994). Specific incorporation of cyclophilin A into HIV-1 virions. Nature *372*, 359–362.

Fuchsova, B., Novak, P., Kafkova, J., and Hozak, P. (2002). Nuclear

DNA helicase II is recruited to IFN-alpha-activated transcription sites at PML nuclear bodies. J. Cell Biol. *158*, 463–473.

Gao, L., Aizaki, H., He, J.W., and Lai, M.M. (2004). Interactions between viral nonstructural proteins and host protein hVAP-33 mediate the formation of hepatitis C virus RNA replication complex on lipid raft. J. Virol. *78*, 3480–3488.

Gosert, R., Egger, D., Lohmann, V., Bartenschlager, R., Blum, H.E., Bienz, K., and Moradpour, D. (2003). Identification of the hepatitis C virus RNA replication complex in Huh-7 cells harboring subgenomic replicons. J. Virol. *77*, 5487–5492.

Grakoui, A., Wychowski, C., Lin, C., Feinstone, S.M., and Rice, C.M. (1993). Expression and identification of hepatitis C virus polyprotein cleavage products. J. Virol. *67*, 1385–1395.

Handschumacher, R.E., Harding, M.W., Rice, J., Drugge, R.J., and Speicher, D.W. (1984). Cyclophilin: a specific cytosolic binding protein for cyclosporin A. Science *226*, 544–547.

Ishii, K., Tanaka, Y., Yap, C.C., Aizaki, H., Matsuura, Y., and Miyamura, T. (1999). Expression of hepatitis C virus NS5B protein: characterization of its RNA polymerase activity and RNA binding. Hepatology *29*, 1227–1235.

Lee, H., Shin, H., Wimmer, E., and Paul, A.V. (2004). cis-acting RNA signals in the NS5B C-terminal coding sequence of the hepatitis C virus genome. J. Virol. *78*, 10865–10877.

Liang, T.J., Jeffers, L.J., Reddy, K.R., De Medina, M., Parker, I.T., Cheinquer, H., Idrovo, V., Rabassa, A., and Schiff, E.R. (1993). Viral pathogenesis of hepatocellular carcinoma in the United States. Hepatology *18*, 1326–1333.

Lohmann, V., Korner, F., Herian, U., and Bartenschlager, R. (1997). Biochemical properties of hepatitis C virus NS5B RNA-dependent RNA polymerase and identification of amino acid sequence motifs essential for enzymatic activity. J. Virol. *71*, 8416–8428.

Lohmann, V., Korner, F., Koch, J., Herian, U., Theilmann, L., and Bartenschlager, R. (1999). Replication of subgenomic hepatitis C virus RNAs in a hepatoma cell line. Science *285*, 110–113.

Loor, F., Tiberghien, F., Wenandy, T., Didier, A., and Traber, R. (2002). Cyclosporins: structure-activity relationships for the inhibition of the human MDR1 P-glycoprotein ABC transporter. J. Med. Chem. *45*, 4598–4612.

Luban, J., Bossolt, K.L., Franke, E.K., Kalpana, G.V., and Goff, S.P. (1993). Human immunodeficiency virus type 1 Gag protein binds to cyclophilins A and B. Cell *73*, 1067–1078.

Miyanari, Y., Hijikata, M., Yamaji, M., Hosaka, M., Takahashi, H., and Shimotohno, K. (2003). Hepatitis C virus non-structural proteins in the probable membranous compartment function in viral genome replication. J. Biol. Chem. *278*, 50301–50308.

Moradpour, D., Brass, V., Bieck, E., Friebe, P., Gosert, R., Blum, H.E., Bartenschlager, R., Penin, F., and Lohmann, V. (2004). Membrane association of the RNA-dependent RNA polymerase is essential for hepatitis C virus RNA replication. J. Virol. *78*, 13278–13284.

Murata, T., Ohshima, T., Yamaji, M., Hosaka, M., Miyanari, Y., Hijikata, M., and Shimotohno, K. (2005). Suppression of hepatitis C virus replicon by TGF-beta. Virology *331*, 407–417.

Nakagawa, M., Sakamoto, N., Enomoto, N., Tanabe, Y., Kanazawa, N., Koyama, T., Kurosaki, M., Maekawa, S., Yamashiro, T., Chen, C.H., et al. (2004). Specific inhibition of hepatitis C virus replication by cyclosporin A. Biochem. Biophys. Res. Commun. *313*, 42–47.

Noueiry, A.O., and Ahlquist, P. (2003). Brome mosaic virus RNA replication: revealing the role of the host in RNA virus replication. Annu. Rev. Phytopathol. *41*, 77–98.

Price, E.R., Jin, M., Lim, D., Pati, S., Walsh, C.T., and McKeon, F.D. (1994). Cyclophilin B trafficking through the secretory pathway is altered by binding of cyclosporin A. Proc. Natl. Acad. Sci. USA *91*, 3931–3935.

Qin, W., Yamashita, T., Shirota, Y., Lin, Y., Wei, W., and Murakami, S. (2001). Mutational analysis of the structure and functions of hepatitis C virus RNA-dependent RNA polymerase. Hepatology *33*, 728–737.

Restrepo-Hartwig, M.A., and Ahlquist, P. (1996). Brome mosaic virus helicase- and polymerase-like proteins colocalize on the endoplasmic reticulum at sites of viral RNA synthesis. J. Virol. *70*, 8908–8916.

Rycyzyn, M.A., and Clevenger, C.V. (2002). The intranuclear prolactin/cyclophilin B complex as a transcriptional inducer. Proc. Natl. Acad. Sci. USA *99*, 6790–6795.

Sanglier, J.J., Quesniaux, V., Fehr, T., Hofmann, H., Mahnke, M., Memmert, K., Schuler, W., Zenke, G., Gschwind, L., Maurer, C., and Schilling, W. (1999). Sanglifehrins A, B, C and D, novel cyclophilin-binding compounds isolated from Streptomyces sp. A92-308110. I. Taxonomy, fermentation, isolation and biological activity. J. Antibiot. (Tokyo) *52*, 466–473.

Schmidt-Mende, J., Bieck, E., Hugle, T., Penin, F., Rice, C.M., Blum, H.E., and Moradpour, D. (2001). Determinants for membrane association of the hepatitis C virus RNA-dependent RNA polymerase. J. Biol. Chem. *276*, 44052–44063.

Schreiber, S.L. (1991). Chemistry and biology of the immunophilins and their immunosuppressive ligands. Science *251*, 283–287.

Schreiber, S.L. (1992). Immunophilin-sensitive protein phosphatase action in cell signaling pathways. Cell *70*, 365–368.

Silverman, J.A., Hayes, M.L., Luft, B.J., and Joiner, K.A. (1997). Characterization of anti-Toxoplasma activity of SDZ 215-918, a cyclosporin derivative lacking immunosuppressive and peptidyl-prolyl-isomerase-inhibiting activity: possible role of a P glycoprotein in Toxoplasma physiology. Antimicrob. Agents Chemother. *41*, 1859–1866.

Takahashi, N. (1999). Pharmacodynamics of ciclosporin A (cyclosporine). Clin. Exp. Nephrol. *3*, S16–S26.

Tellinghuisen, T.L., and Rice, C.M. (2002). Interaction between hepatitis C virus proteins and host cell factors. Curr. Opin. Microbiol. *5*, 419–427.

Thali, M., Bukovsky, A., Kondo, E., Rosenwirth, B., Walsh, C.T., Sodroski, J., and Gottlinger, H.G. (1994). Functional association of cyclophilin A with HIV-1 virions. Nature *372*, 363–365.

Towers, G.J., Hatziioannou, T., Cowan, S., Goff, S.P., Luban, J., and Bieniasz, P.D. (2003). Cyclophilin A modulates the sensitivity of HIV-1 to host restriction factors. Nat. Med. *9*, 1138–1143.

Waldmeier, P.C., Zimmermann, K., Qian, T., Tintelnot-Blomley, M., and Lemasters, J.J. (2003). Cyclophilin D as a drug target. Curr. Med. Chem. *10*, 1485–1506.

Watashi, K., Hijikata, M., Marusawa, H., Doi, T., and Shimotohno, K. (2001). Cytoplasmic localization is important for transcription factor nuclear factor-kappa B activation by hepatitis C virus core protein through its amino terminal region. Virology *286*, 391–402.

Watashi, K., Hijikata, M., Hosaka, M., Yamaji, M., and Shimotohno, K. (2003a). Cyclosporin A suppresses replication of hepatitis C virus genome in cultured hepatocytes. Hepatology *38*, 1282–1288.

Watashi, K., Hijikata, M., Tagawa, A., Doi, T., Marusawa, H., and Shimotohno, K. (2003b). Modulation of retinoid signaling by a cytoplasmic viral protein via sequestration of Sp110b, a potent transcriptional corepressor of retinoic acid receptor, from the nucleus. Mol. Cell. Biol. *23*, 7498–7509.

Wu, J.Z., and Hong, Z. (2003). Targeting NS5B RNA-dependent RNA polymerase for anti-HCV chemotherapy. Curr. Drug Targets Infect. Disord. *3*, 207–219.

You, S., Stump, D.D., Branch, A.D., and Rice, C.M. (2004). A cis-acting replication element in the sequence encoding the NS5B RNA-dependent RNA polymerase is required for hepatitis C virus RNA replication. J. Virol. *78*, 1352–1366.

Available online at www.sciencedirect.com
SCIENCE DIRECT
Biochemical and Biophysical Research Communications 340 (2006) 792–799
BBRC
www.elsevier.com/locate/ybbrc

Single-point mutations of hepatitis C virus NS3 that impair p53 interaction and anti-apoptotic activity of NS3 ☆

Motofumi Tanaka, Motoko Nagano-Fujii, Lin Deng, Satoshi Ishido [1], Kiyonao Sada, Hak Hotta *

Division of Microbiology, Kobe University Graduate School of Medicine, Kobe 650-0017, Japan

Received 16 November 2005
Available online 20 December 2005

Abstract

The N-terminal domain of NS3 of hepatitis C virus (HCV) possesses serine protease activity, which is essential for virus replication. This portion is also implicated in malignant transformation of hepatocytes. We previously demonstrated that an N-terminal portion of NS3 formed a complex with the tumor suppressor p53 and suppressed actinomycin D-induced apoptosis. We report here that single-point mutations of NS3 at position 106 from Leu to Ala (L106A), and position 43 from Phe to Ala (F43A) to a lesser extent, significantly impaired complex formation with p53. Moreover, the L106A mutation impaired an otherwise more distinct anti-apoptotic activity of NS3. F43A and L106A mutations also inhibited serine protease activity of NS3. These results collectively suggest the possibility that Leu^{106} and Phe^{43} are involved in p53 interaction and serine protease activity, and therefore, can be a good target for certain low-molecular-weight compound(s) to inhibit both oncogenic and replicative abilities of HCV.

Keywords: Hepatitis C virus; NS3; p53; Tumor suppressor; Protein-protein interaction; Point mutation; Apoptosis; Serine protease

Hepatitis C virus (HCV) was identified as the major etiological agent of most transfusion-associated non-A, non-B hepatitides in 1989 [1,2]. It has been estimated that more than 170 million people are infected with HCV worldwide [3]. HCV easily establishes persistent infection, which may be mild, or sometimes even asymptomatic, in early phases of the disease, but after a decade or two, may cause liver cirrhosis and eventually hepatocellular carcinoma [4].

HCV, an enveloped RNA virus, belongs to genus *Hepacivirus*, family *Flaviviridae* [5]. The viral genome, single-stranded, positive-sense RNA of about 9.6 kb, consists of 5′- and 3′-untranslated regions, and a large open-reading frame that encodes a polyprotein precursor of 3010–3030 amino acids (aa) [5,6]. The polyprotein is cleaved by the host signal peptidase and virus-encoded two proteases to generate mature viral proteins; four structural proteins, such as Core, E1, E2, p7, and six non-structural proteins, such as NS2, NS3, NS4A, NS4B, NS5A, and NS5B [5,7,8].

HCV NS3 is a multifunctional protein essential for virus replication. Its N-terminal one-third is responsible for chymotrypsin-like serine protease activity that cleaves at the NS3/4A, NS4A/4B, NS4B/5A, and NS5A/5B junctions [9,10]. A minimal portion of the NS3 serine protease activity has been mapped to a region between aa 33 and 178 [11]. Its C-terminal half possesses RNA helicase activity [9,10]. In addition to its important roles in virus replication, NS3 is implicated in malignant transformation. For example, an N-terminal portion of NS3 was reported to transform NIH3T3 cells [12] and rat fibroblast cells [13].

☆ *Abbreviations:* HCV, hepatitis C virus; aa, amino acid; GST, glutathione *S* transferase; PBS, phosphate-buffered saline; wt, wild-type; mut, mutant-type.

* Corresponding author. Fax: +81 78 382 5519.
E-mail address: hotta@kobe-u.ac.jp (H. Hotta).
[1] Present address: Laboratory for Infectious Immunity, Riken Research Center for Allergy and Immunology, Yokohama, Kanagawa 230-0045, Japan.

0006-291X/$ - see front matter © 2005 Elsevier Inc. All rights reserved.
doi:10.1016/j.bbrc.2005.12.076

We also observed that an N-terminal portion of NS3 inhibited apoptosis of NIH3T3 cells [14], which is a prerequisite for malignant transformation.

The tumor suppressor p53 is a key molecule in the signaling pathway of apoptosis induced by DNA damage or deregulated cell cycle [15]. Some DNA tumor viruses are known to interact with p53 to inactivate its function. For example, human papillomavirus E6 forms a ternary complex with p53 and E6AP, an E3 ubiquitin ligase, and this complex formation results in the ubiquitination and subsequent degradation of p53 [16,17]. It has also been demonstrated that simian virus 40 T antigen binds to and inactivates the function of p53 [18]. Similarly, adenovirus E1B [19] and hepatitis B virus X protein [20] were reported to suppress p53 function although their direct binding to p53 appears to be weak.

As for the possible interaction between HCV NS3 and p53, it was reported that NS3 repressed p53-dependent transcriptional activity of $p21^{waf1}$ [21]. Also, we have demonstrated that p53 enhances nuclear accumulation of NS3 [22,23] and that NS3, through its N-terminal portion, forms a complex with p53 [24]. In this study, we defined a minimum p53-binding region(s) of NS3 and identified single-point mutations that impaired the interaction with p53. We also examined possible biological significance of those mutations.

Materials and methods

Expression plasmids. cDNA encoding an N-terminal region of NS3 (aa 1–198) of the HCV isolate no. 43 [25] (GenBank Accession No. AB072085) was amplified using primers NS3/M/B and NS3/AS/H (Table 1), and subcloned into pcDNA3.1/Myc-His(-)C (pcDNA) (Invitrogen) to generate pcDns3/1–198. Various deletion mutants of pcDns3/1–198 (see Fig. 1A) were constructed using appropriate sets of primers, NS3-del-S and NS3-del-AS. To express the full-length NS3 (NS3-Full), the entire NS3 sequence was amplified from pBSns3/1–631 [23] (GenBank Accession No. D45172) using primers NS3/M/B and NS3F/HindIII, and subcloned into pcDNA. The resultant plasmid was designated pcDns3-Full. All the NS3 fragments expressed from these plasmids could be detected by anti-Myc antibody. Expression plasmids for NS3 fragments tagged with glutathione *S* transferase (GST) and Myc-His were also constructed. In brief, *Hin*cII–*Bam*HI fragment of pGEX-4T-1 (Amersham Biosciences) containing GST sequence was subcloned into pBlueScript II SK- to generate pBS-GST. An *Eco*RI–*Bam*HI fragment of pBS-GST was introduced to pcDNA to generate pcDgst. Various deletion mutants of NS3 were amplified from pcDns3/1–198 and subcloned into pcDgst.

Single-point mutations were introduced using QuikChange Site-Directed Mutagenesis kit (Stratagene) according to the manufacturer's instruction. For plasmid-based expression, the Myc-tagged NS3 fragments described above were subcloned into pSG5 vector (Stratagene) downstream of simian virus 40 early promoter.

An expression plasmid for Myc-tagged NS4B, designated pEFns4B, was constructed by amplifying the corresponding sequence from pM094AJ (HCV-1b) [26] using primers NS4B-1-S and NS4B-Xba-AS, and subcloned into pEF1/Myc-His (Invitrogen). A coding region for NS5A/5BΔC polyprotein (aa 1973–2721 in the entire HCV polyprotein) was amplified from pTMns2-5b(810–2721) [23] using primers 5A5BncoI and 5A5BpstI, and subcloned into pTM1 vector to generate pTM-NS5A/5BΔC. This plasmid was used to express a substrate for the NS3 serine protease.

To express p53, *Xho*I fragments of pcDM8VAarg/neo and pcDM8A431/neo [22,23,27], which harbor the entire sequences of wild-type (wt) and mutant-type (mut) p53, respectively, were subcloned into pcDNA and pSG5 vectors. Resultant plasmids were designated pcDwt-p53, pcDmut-p53, and pSGwt-p53. pSGwt-p53 was used for plasmid-based expression.

Transient protein expression. HeLa and Huh7 cells were maintained in Dulbecco's modified Eagle's medium supplemented with 10% heat-inactivated fetal bovine serum at 37 °C in 5% CO_2. For protein expression, vaccinia virus-T7 hybrid expression and plasmid-based expression systems were used, as reported previously [22–24,28]. After overnight cultivation, the protein expression was examined by the following analyses.

Immunoprecipitation and immunoblotting. Cells were lysed in a buffer consisting of 10 mM Tris–HCl (pH 7.5), 150 mM NaCl, 1% Triton X-100, and 1 mM EDTA. After being clarified by centrifugation, cell lysates were incubated with anti-p53 rabbit antiserum (Santa Cruz) for 1 h at 4 °C and then further incubated with protein A–Sepharose beads (Amersham) on a rotator for 30 min at 4 °C. Normal rabbit serum served as a control. After being washed with the buffer, the immunoprecipitates were subjected to SDS–PAGE and blotted onto a polyvinylidene fluoride membrane (Immobilon-P, Millipore). After being blocked with 5% skim milk, the membrane was incubated with mouse monoclonal antibody against either the Myc peptide (Santa Cruz Biotechnol.) or p53 (Ab-1; Calbiochem) and subsequently with peroxidase-labeled goat anti-mouse IgG (MBL, Nagoya, Japan). The protein bands were visualized by using an enhanced chemiluminescence (Amersham) and their intensity was measured by LAS-1000 (Fuji Film).

Double-staining immunofluorescence. Cells were fixed with 3.7% paraformaldehyde for 15 min at 37 °C and cold methanol for 10 min. After being washed with phosphate-buffered saline (PBS), the cells were incubated with anti-Myc mouse monoclonal antibody (Santa Cruz) and anti-p53 rabbit antiserum (Santa Cruz) for 1 h. The cells were washed with PBS and then incubated with FITC-conjugated goat anti-mouse IgG (MBL)

Table 1
Oligonucleotide primers used for PCR amplification

Primer	Sequence[a]	Amplified direction
NS3/M/B	5′-GCAAGGATCCGCCATGGCGCCTATCACGGCCTA-3′	Forward
NS3/AS/H	5′-CTCCAAGCTTGGAATGTTTGCGGTA-3′	Reverse
NS3FHindIII	5′-CTCCAAGCTTGAGTGACCTCTAGGT-3′	Reverse
NS3-del-S[b]	5′-GCAAGAATCCGCCATG $(N)_{15-18}$-3′	Forward
NS3-del-AS[b]	5′-$(n)_4$AAGCTTC $(N)_{13-18}$-3′	Reverse
NS4B-1-S	5′-CCGCGAATTCAACATGGCGTGGAGCAGTC-3′	Forward
NS4B-Xba-AS	5′-TATATCTAGACATGGCGTGGAGCAG-3′	Reverse
5A5BNcoI	5′-CCACCATGGGCTCCGGCTCGTGGCTCAG-3′	Forward
5A5BpstI	5′-CAGGCTGCAGAGGCCTTCAAGTAACATGTG-3′	Reverse

[a] Restriction enzyme recognition sites are underlined. The translation initiation codon is shown in boldface letters.

[b] A group of primers used to amplify various deletion mutants of NS3 (see Fig. 1A). N, nucleotide residues either identical or complementary to those of the isolate no. 43 [25] (GenBank Accession No. AB072085); *n*, arbitrarily added residues that help ensure the recognition of the following sequences by the respective restriction enzymes.

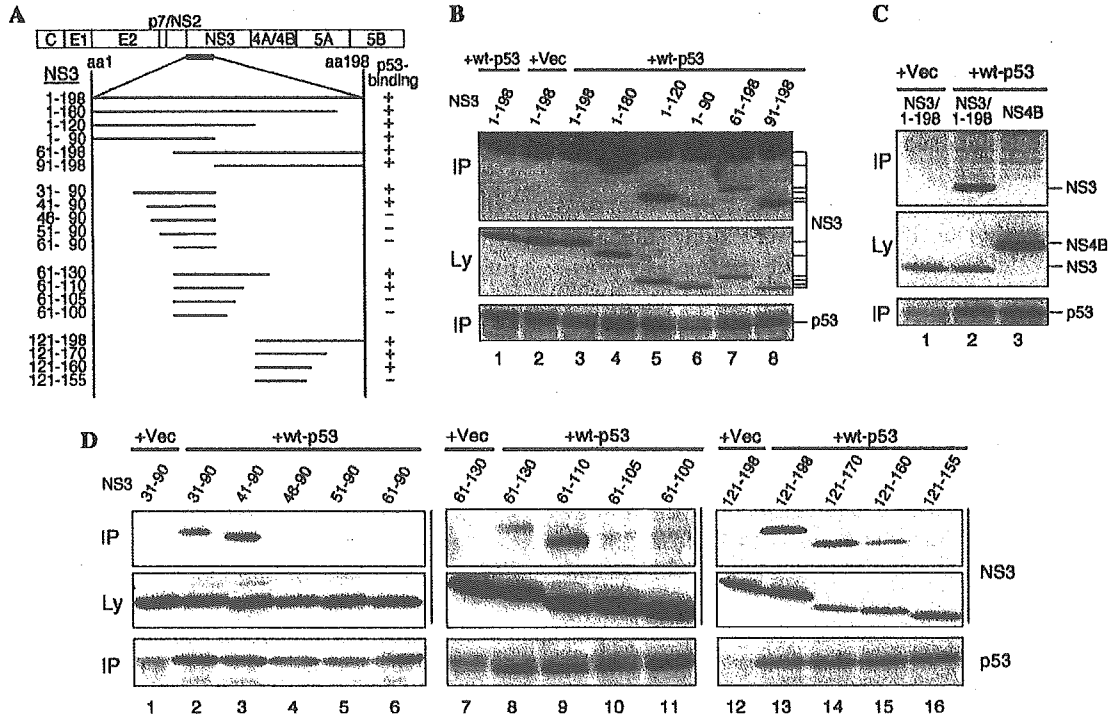

Fig. 1. Minimum regions of NS3 responsible for complex formation with wt-p53. (A) Schematic diagram of the HCV genome and NS3. NS3-Full, NS3/1–198, and various deletion mutants are depicted. (B) Various deletion mutants of Myc-tagged NS3 were expressed without (lane 2) or with wt-p53 (lanes 1 and 3–8) in HeLa cells by using vaccinia-T7 hybrid expression method. Cell lysates were immunoprecipitated using anti-p53 rabbit antiserum (lanes 2–8) or with normal rabbit IgG (lane 1), and the immunoprecipitates were probed with anti-Myc antibody to detect NS3 (upper panel). The lysates were directly (without being immunoprecipitated with anti-p53 antibody) probed with anti-Myc antibody to verify comparable degrees of expression of the NS3 mutants (middle panel). Efficient immunoprecipitation of wt-p53 with anti-p53 antibody was also verified (lower panel). (C) Myc-tagged NS3/1–198 and full-length NS4B were each co-expressed with wt-p53. Cells expressing NS3 alone (lane 1) were also prepared. Cell lysates were immunoprecipitated with anti-p53 antibody, and the immunoprecipitates were probed with anti-Myc antibody (upper panel). The lysates were directly probed with anti-Myc antibody to verify the expression of NS3/1–198 and NS4B (middle panel). Efficient immunoprecipitation of wt-p53 was also verified (lower panel). (D) NS3 mutants tagged with GST and Myc were expressed without (lanes 1, 7, and 12) or with wt-p53 (lanes 2–6, 8–11, and 13–16). Cell lysates were immunoprecipitated using anti-p53 antibody and then probed with anti-Myc antibody (upper panel). The lysates were directly probed with anti-Myc antibody (middle panel). Efficient immunoprecipitation of wt-p53 was also verified (lower panel).

and Cy3-conjugated donkey anti-rabbit IgG (Chemicon) for another 1 h. The cells were observed with a laser scanning confocal microscope (Carl Zeiss).

NS3-expressing cell lines. NIH3T3 cells were maintained in Dulbecco's modified Eagle's medium containing 10% heat-inactivated fetal calf serum at 37 °C in a CO_2 incubator, as described previously [14]. The cells were transfected with pSGns3/1–180, pSGns3/1–180/L106A, or the pSG5 empty vector, together with pSV2-neo as a selection marker, and cultivated in the presence of a neomycin derivative (G418, 600 μg/ml, Gibco). After 2 weeks, stable transformants were cloned using cloning cylinders and tested for NS3 expression by immunoblotting. Five clones each strongly expressing NS3/1–180 or NS3/1–180/L106A, and the non-expressing control, were selected and mixed to avoid clonal variation.

Quantitative apoptosis assays. Cells were seeded into 6-mm well of a 96-well plate at a concentration of 5×10^3 cells/well and incubated overnight. The cells were then treated with actinomycin D (10 ng/ml) for 3 days. The number of living cells was monitored every day by using cell proliferation reagent WST-1 (Roche), according to the manufacturer's protocol. In brief, 100 μl of culture medium containing 10% WST-1 was added to each well. After 1 h, the absorbance was measured at 450 nm with a microplate reader.

Measurement of serine protease activity of NS3. Various forms of NS3 were co-expressed with NS5A/5BΔC polyprotein, a substrate for the NS3 serine protease. The cells were lysed, probed, and subjected to immunoblot analysis using anti-NS5A mouse monoclonal antibody (kindly provided by I. Yoshida, Research Institute for Microbial Diseases, Kan-Onji Branch, Kagawa, Japan) and peroxidase-conjugated goat anti-mouse IgG (MBL). Intensity of the bands corresponding to the cleaved NS5A and the uncleaved NS5A/5BΔC was measured. Arbitrary units of serine protease activity of each NS3 were calculated by the following formula:

$$\text{Protease activity (arbitrary unit)} = \text{NS5A} \div (\text{NS5A/5B}\Delta C + \text{NS5A}).$$

Results

Minimum regions of NS3 responsible for complex formation with p53

We previously demonstrated that an N-terminal portion of NS3 (aa 29–174) was involved in complex formation with wt-p53 [24]. In this study, we aimed to narrow down the p53-binding region(s) and to determine a residue(s) responsible for the interaction. We expressed a number of deletion mutants of NS3 (Fig. 1A). Initial immunoprecipitation experiments revealed that two non-overlapping regions of NS3, one spanning from 1 to 90 and the other from 91 to 198, each formed a complex with p53

(Fig. 1B, lanes 6 and 8). The specificity of the interaction between NS3 and p53 was secured by control experiments (lanes 1 and 2) and also confirmed by the lack of interaction between p53 and a control protein, HCV NS4B (Fig. 1C). These results suggested the possible presence of at least two separate regions responsible for p53 binding. We then tried to express further deleted NS3 sequences. However, those shorter fragments were quite unstable and only poorly detectable, which made the analysis practically impossible. Therefore, we expressed NS3 fragments tagged with GST and Myc-His to overcome this problem.

GST- and/or Myc-tagged NS3 fragments used in this study are shown in Fig. 1A. Using these fragments, we identified three separate regions; NS3/41–90, /61–110, and /121–160 forming a complex with p53 (Fig. 1D, lanes 3, 9, and 15). On the other hand, NS3/46–90, /61–105, and /121–155 fail to interact with p53 (lanes 4, 10, and 16), suggesting that residues at positions from 41 to 45, from 106 to 110, and from 156 to 160 were likely to be involved in the interaction.

To identify the responsible residues, we introduced a single-point mutation and tested the ability of each NS3 mutant to interact with p53. The results clearly demonstrated that a single-point mutation of NS3 at position 43 from Phe to Ala (F43A) abolished the interaction with p53 (Fig. 2, lane 5). Likewise, single-point mutations at position 106 from Leu to Ala (L106A) and position 158 from Val to Ala (V158A) abolished the interaction with p53 (lanes 9 and 15). These results obtained with GST- and Myc-tagged short fragments of NS3 suggested the possible importance for Phe, Leu, and Val at positions 43, 106, and 158, respectively, in complex formation with p53.

Residues of NS3 responsible for complex formation with p53

We then introduced the F43A and L106A mutations into Myc-tagged NS3/1–180 and NS3-Full, and examined their possible interaction with p53. The results obtained demonstrated that the introduction of L106A mutation into NS3/1–180 markedly inhibited interaction with p53 while F43A mutation only weakly impaired it (Fig. 3A). On the other hand, V158A mutation did not affect the interaction (data not shown). When introduced to NS3-Full, L106A mutation, again, markedly inhibited interaction with p53 while F43A mutation only weakly (Fig. 3B). These results suggested an important role for Leu at position 106, and Phe at position 43 to a lesser extent, in the interaction between NS3 and p53.

We also examined the possible effect of those single-point mutations on the interaction with mut-p53, which has a mutation at position 273 from Arg to Gln and, unlike wt-p53, localizes exclusively in the cytoplasm [22]. The result showed that, when introduced to NS3/1–180, L106A mutation markedly impaired the interaction with mut-p53 (Fig. 3C). F43A mutation also impaired the interaction with mut-p53, though to a lesser extent than that observed with the L106A mutation. These results are consistent with those obtained with wt-p53 (see Fig. 3A).

Effects of single-point mutations on subcellular localization of NS3 in the presence and absence of wt-p53

We have reported that NS3-Full and its C-terminally truncated form (NS3/1–433) were each co-localized with wt-p53 almost exclusively in the nucleus when transiently expressed in HeLa cells [22,23]. In this study, we investigated the subcellular localization of NS3/1–180, NS3-Full, and their point mutants both in the presence and absence of wt-p53 in Huh7 cells using plasmid-based expression system. NS3/1–180 was localized both in the cytoplasm and the nucleus when expressed alone (Fig. 4a), and was localized almost exclusively in the nucleus when co-expressed with wt-p53 (Figs. 4b–d), with the results being consistent with our previous observations [22,23]. NS3/1–180/F43A exhibited practically the same localization patterns as those of the parental NS3/1–180 both in the absence and presence of wt-p53 co-expression (Figs. 4e–h). However, NS3/1–180/L106A was localized exclusively in the cytoplasm, exhibiting a dot-like pattern, irrespective of p53 co-expression (Figs. 4i–l). Similar results were obtained when L106A mutation was introduced into NS3-Full; unlike the wild-type NS3-Full (Figs. 4m–p), the L106A mutant showed exclusive cytoplasmic localization, irrespective of wt-p53

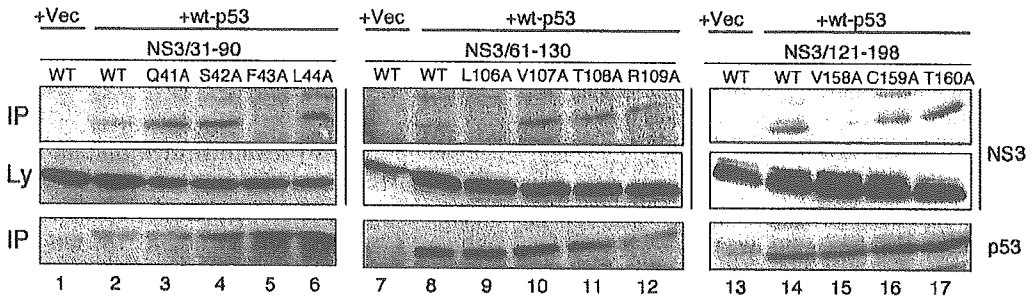

Fig. 2. Single-point mutations of NS3 responsible for complex formation with wt-p53. GST- and Myc-tagged NS3/31–90, NS3/61–130, NS3/121–198, and their single-point mutants were expressed in HeLa cells without (lanes 1, 7, and 13) or with wt-p53 (lanes 2–6, 8–12, and 14–17). Cell lysates were immunoprecipitated using anti-p53 antibody and probed with anti-Myc antibody to detect NS3 (upper panel). The lysates were directly probed with anti-Myc antibody (middle panel). Efficient immunoprecipitation of wt-p53 was also verified (lower panel). WT, wild-type (without point mutation).

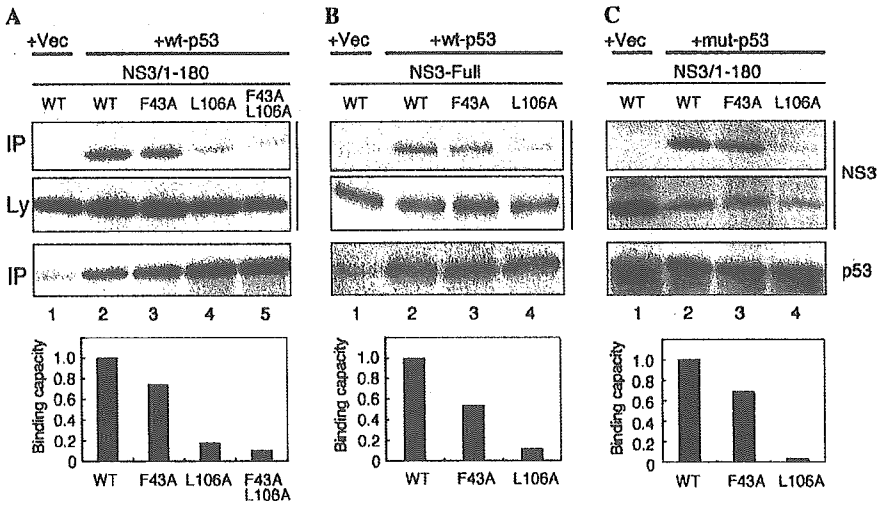

Fig. 3. F43A and L106A mutations in NS3/1–180 and NS3-Full impair complex formation with wt-p53. (A) Myc-tagged NS3/1–180 and its point mutants were expressed in HeLa cells without (lane 1) or with wt-p53 (lanes 2–5). Cell lysates were immunoprecipitated using anti-p53 antibody and probed with anti-Myc antibody to detect NS3 (upper panel). The lysates were directly probed with anti-Myc antibody (middle panel). Efficient immunoprecipitation of wt-p53 was also verified (lower panel). Amounts of NS3 co-immunoprecipitated with p53 were normalized to the total amounts of NS3 in the lysates. The normalized values, considered as p53-binding capacity of NS3, are depicted in the graph (bottom). (B) Similar analysis was performed using NS3-Full. (C) Similar analysis was performed using mut-p53 and NS3/1–180. WT, wild-type (without point mutation).

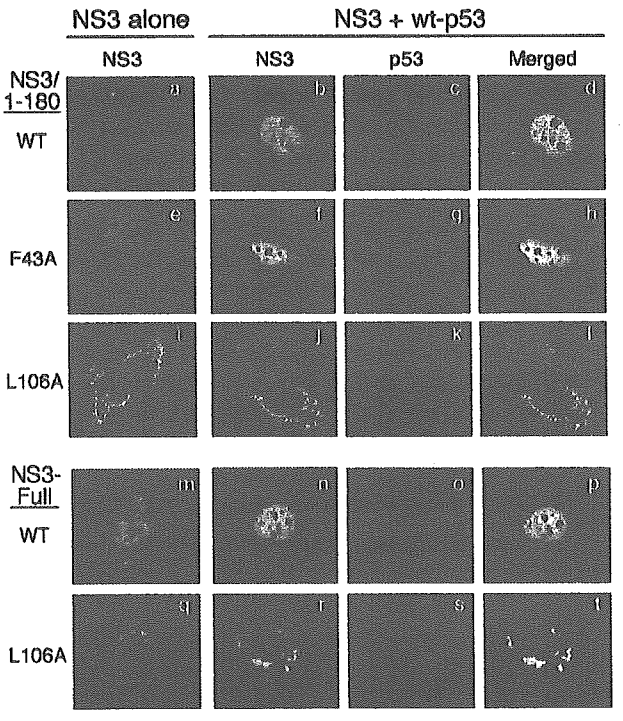

Fig. 4. L106A, but not F43A, mutation alters subcellular localization of NS3/1–180 and NS3-Full in the presence of wt-p53. NS3/1–180, NS3-Full, and their single-point mutants were each expressed without or with wt-p53 in Huh7 cells by plasmid-based expression system. The cells were stained with anti-Myc mouse monoclonal antibody and anti-p53 rabbit antiserum, followed by FITC-conjugated anti-mouse IgG (green) and Cy3-conjugated anti-rabbit IgG (red). Merged pictures are shown on the right. WT, wild-type (without point mutation).

co-expression (Figs. 4q–t). Similar localization patterns of NS3/1–180, NS3-Full, and their point mutants in the presence and absence of wt-p53 were consistently observed using vaccinia virus-T7 hybrid expression system in HeLa cells (data not shown).

Impairment of anti-apoptotic activity of NS3 by the L106A mutation

Cells were treated with actinomycin D for 3 days and examined for apoptosis. Consistent with our previous observations with a longer NS3 sequence encoding aa 1–433 [14], cells stably expressing NS3/1–180 showed a higher degree of resistance against actinomycin D-induced apoptosis than the non-expressing control. The otherwise distinct anti-apoptotic activity of NS3 was significantly impaired by the L106A mutation (Fig. 5). Significant impairment of NS3 anti-apoptotic activity by the L106A mutation was also evident 2 days after actinomycin D treatment (data not shown). Similar results were reproducibly obtained in separate experiments.

Effects of single-point mutations on serine protease activity of NS3

The NS3 serine protease cleaves NS5A/5BΔC polyprotein into two fragments, NS5A and NS5BΔC. By using this system, we compared serine protease activities of various single-point mutants of NS3. As shown in Fig. 6A, introduction of either F43A or L106A mutation into NS3/1–180 markedly impaired the otherwise strong serine protease activity whereas the inhibitory effect of V158A mutation was marginal. Similarly, when introduced into

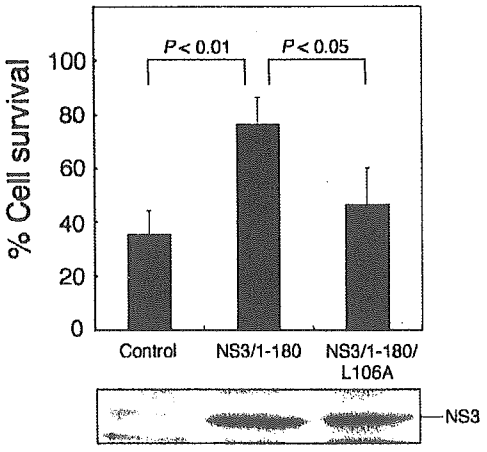

Fig. 5. L106A mutation impairs anti-apoptotic activity of NS3/1–180. Percent cell survival after actinomycin D treatment (10 ng/ml, 3 days) is shown. Data represent means ± SD obtained from triplicate cultures of two independent experiments. Expression levels of NS3/1–180 and its L106A mutant in mixed cultures of five clones each are shown at the bottom.

NS3-Full, L106A mutation markedly impaired the serine protease activity while F43A mutation impaired it moderately (Fig. 6B).

Discussion

We demonstrated in the present study that single-point mutations of NS3, either NS3/1–180 or NS3-Full, at position 106 from Leu to Ala (L106A), and position 43 from Phe to Ala (F43A) to a lesser extent, inhibited complex formation with p53 (Fig. 3). We previously reported that a 146-residue fragment near the N-terminus of NS3 (aa 29–174) was involved in the interaction with p53 [22–24]. We also noticed that secondary structure of the N-terminal 120 residues of NS3 was well correlated with the risk for development of hepatocellular carcinoma in HCV-infected patients [25]. These results suggest an important role for the N-terminal portion of NS3, especially Phe and Leu at positions 43 and 106, respectively, in the pathogenesis of HCV, such as anti-apoptotic status [14], a mutation-prone phenotype [29,30], malignant transformation of cultured cells [12,13], and eventually development of hepatocellular carcinoma in patients [25]. We previously reported that N-terminal two-thirds of NS3 (aa 1–433) inhibited actinomycin D-induced apoptosis [14]. In the present study, we observed that even a shorter NS3 fragment, NS3/1–180, inhibited actinomycin D-induced apoptosis and that the L106A mutation significantly impaired otherwise more distinct anti-apoptotic activity of NS3/1–180 (Fig. 5). Our results collectively suggest the possibility that the L106A mutation impairs NS3 anti-apoptotic activity through decreased p53 binding.

Inhibition of apoptosis is a prerequisite for malignant transformation of the cell. However, another cellular event(s) is required for malignant transformation. In fact, we observed that, despite distinct inhibition of apoptosis, NIH3T3 cells stably expressing the N-terminal two-thirds of NS3 [14] or NS3/1–180 (data not shown) did not exhibit typical malignant phenotypes, such as higher population density in anchorage-dependent culture, colony formation in anchorage-independent culture, and tumor formation in nude mice. Our results appear to be inconsistent with a previous report by other researchers that an N-terminal portion of NS3 flanked with a short stretch of a C-terminal portion of NS2-mediated malignant transformation of

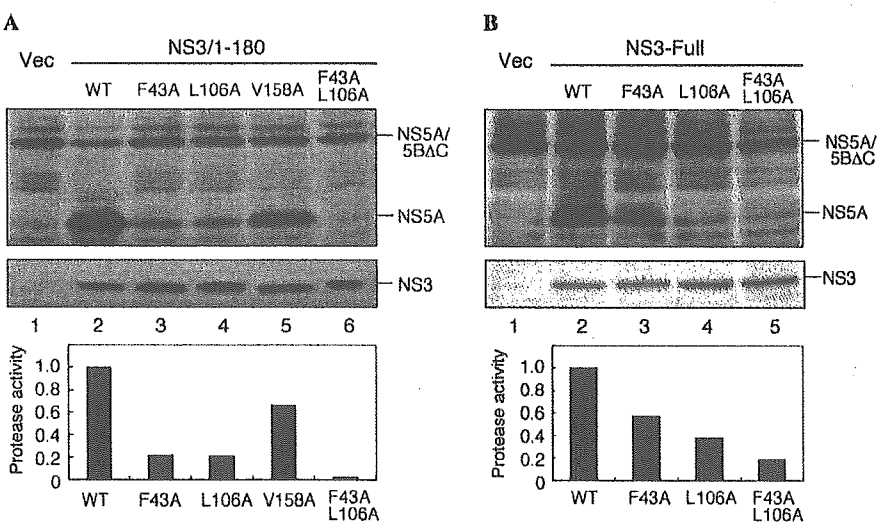

Fig. 6. F43A and L106A mutations in NS3/1–180 and NS3-Full impair the serine protease activity. (A) NS5A/5BΔC, a substrate for NS3 serine protease, was expressed in HeLa cells without (lane 1) or with Myc-tagged NS3/1–180 (lane 2) and its point mutants (lanes 3–6). Cell lysates were probed with anti-NS5A antibody to detect uncleaved and cleaved NS5A fragments (upper panel). The lysates were also probed with anti-Myc antibody to verify a comparable degree of NS3 expression in each lane (lower panel). Serine protease activities were measured, as described in Materials and methods, and are depicted in the graph (bottom). (B) Similar analysis was performed using NS3-Full.

NIH3T3 cells [12]. This discrepancy might be explained by the differences in aa sequences and expression levels of NS3, and/or cellular characteristics, etc. Further studies are needed to fully understand the mechanism of malignant transformation by HCV.

L106A and F43A mutations also inhibited serine protease activity of NS3 (Fig. 6). Due to the impairment of the enzymatic activity essential for virus replication [5], HCV strains with such a mutation(s) would not replicate efficiently and, therefore, they would become less prevalent in a patient population. Indeed, we have not found the F43A or L106A mutations among ~200 HCV clinical isolates so far tested [25].

Crystal structure analysis of the serine protease domain of NS3 reported previously [31,32] suggests that the residues at positions 43 and 106 are localized spatially in the close proximity to Ser at position 139, one of the catalytic triads of NS3 serine protease activity. This may explain why a single-point mutation, such as L106A, impairs two unrelated NS3 properties, p53-binding and serine protease activity. These results collectively imply the possibility that certain low-molecular-weight compound(s) that specifically interact with the residues at position 106 or 43 interfere with both oncogenic and replicative abilities of HCV.

Acknowledgments

We thank Dr. I. Yoshida, Research Institute for Microbial Diseases, Kan-Onji Branch, Kagawa, Japan, for providing anti-NS5A monoclonal antibody. This study was supported in part by Grants-in-Aid for Scientific Research from the Ministry of Education, Culture, Sports, Science and Technology, Japan Society for the Promotion of Science, and the Ministry of Health, Labour and Welfare, Japan. This study was also carried out as part of the 21COE Program at Kobe University Graduate School of Medicine.

References

[1] G. Kuo, Q.-L. Choo, H.J. Alter, G.L. Gitnick, A.G. Redeker, R.H. Purcell, T. Miyamura, J.L. Dienstag, M.J. Alter, C.E. Stevens, G.E. Tegtmeier, F. Bonino, M. Colombo, W.-S. Lee, C. Kuo, K. Berger, J.R. Shuster, L.R. Overby, D.W. Bradley, M. Houghton, An assay for circulating antibodies to a major etiologic virus of human non-A, non-B hepatitis, Science 244 (1989) 362–364.

[2] Q.-L. Choo, G. Kuo, A.J. Weiner, L.R. Overby, D.W. Bradley, M. Houghton, Isolation of a cDNA clone derived from a blood-borne non-A, non-B viral hepatitis genome, Science 244 (1989) 359–362.

[3] World Health Organization, Wkly. Epidemiol. Rec. 74 (1999) 425–427.

[4] I. Saito, T. Miyamura, A. Ohbayashi, H. Harada, T. Katayama, S. Kikuchi, Y. Watanabe, S. Koi, M. Onji, Y. Ohta, Q.-L. Choo, M. Houghton, G. Kuo, Hepatitis C virus infection is associated with the development of hepatocellular carcinoma, Proc. Natl. Acad. Sci. USA 87 (1990) 6547–6549.

[5] K.E. Reed, C.M. Rice, Overview of hepatitis C virus genome structure, polyprotein processing, and protein properties, Curr. Top. Microbiol. Immunol. 242 (2000) 55–84.

[6] N. Kato, M. Hijikata, Y. Ootsuyama, M. Nakagawa, S. Ohkoshi, T. Sugimura, K. Shimotohno, Molecular cloning of the human hepatitis C virus genome from Japanese patients with non-A, non-B hepatitis, Proc. Natl. Acad. Sci. USA 87 (1990) 9524–9528.

[7] Q.-L. Choo, K.H. Richman, J.H. Han, K. Berger, C. Lee, C. Dong, C. Gallegos, D. Coit, A. Medina-Selby, P.J. Barr, A.J. Weiner, D.W. Bradley, G. Kuo, M. Houghton, Genetic organization and diversity of the hepatitis C virus, Proc. Natl. Acad. Sci. USA 88 (1991) 2451–2455.

[8] M. Hijikata, N. Kato, Y. Ootsuyama, M. Nakagawa, K. Shimotohno, Gene mapping of the putative structural region of the hepatitis C virus genome by in vitro processing analysis, Proc. Natl. Acad. Sci. USA 88 (1991) 5547–5551.

[9] Y. Tanji, M. Hijikata, S. Satoh, T. Kaneko, K. Shimotohno, Hepatitis C virus-encoded nonstructural protein NS4A has versatile functions in viral protein processing, J. Virol. 69 (1995) 1575–1581.

[10] R. Bartenschlager, V. Lohmann, T. Wilkinson, J.O. Koch, Complex formation between the NS3 serine-type proteinase of the hepatitis C virus and NS4A and its importance for polyprotein maturation, J. Virol. 69 (1995) 7519–7528.

[11] K. Yamada, A. Mori, M. Seki, J. Kimura, S. Yuasa, Y. Matsuura, T. Miyamura, Critical point mutations for hepatitis C virus NS3 proteinase, Virology 246 (1998) 104–112.

[12] D. Sakamuro, T. Furukawa, T. Takegami, Hepatitis C virus nonstructural protein NS3 transform NIH3T3 cells, J. Virol. 69 (1995) 3893–3896.

[13] R. Zemel, S. Gerechet, H. Greif, L. Bachmatove, Y. Birk, A. Golan-Goldhirsh, M. Kunin, Y. Berdichevsky, I. Benhar, R. Tur-Kaspa, Cell transformation induced by hepatitis C virus NS3 serine protease, J. Viral Hepat. 8 (2001) 96–102.

[14] T. Fujita, S. Ishido, S. Muramatsu, M. Itoh, H. Hotta, Suppression of actinomycin D-induced apoptosis by the NS3 protein of hepatitis C virus, Biochem. Biophys. Res. Commun. 229 (1996) 825–831.

[15] A.J. Levine, p53, the cellular gatekeeper for growth and division, Cell 88 (1997) 323–331.

[16] K. Münger, P.M. Howley, Human papillomavirus immortalization and transformation functions, Virus Res. 89 (2002) 213–228.

[17] M.S. Longworth, L.A. Laimins, Pathogenesis of human papillomaviruses in differentiating epithelia, Microbiol. Mol. Biol. Rev. 68 (2004) 362–372.

[18] C.S. Sullivan, J.M. Pipas, T antigens of simian virus 40: molecular chaperones for viral replication and tumorigenesis, Microbiol. Mol. Biol. Rev. 66 (2002) 179–202.

[19] C. Endter, T. Dobner, Cell transformation by human adenoviruses, Curr. Top. Microbiol. Immunol. 273 (2004) 163–214.

[20] S. Murakami, Hepatitis B virus X protein: a multifunctional viral regulator, J. Gastroenterol. 36 (2001) 651–660.

[21] H.J. Kwun, E.Y. Jung, J.Y. Ahn, M.N. Lee, K.L. Jang, p53-dependent transcriptional repression of $p21^{waf1}$ by hepatitis C virus NS3, J. Gen. Virol. 82 (2001) 2235–2241.

[22] S. Ishido, S. Muramatsu, T. Fujita, Y. Iwanaga, W.-Y. Tong, Y. Katayama, M. Itoh, H. Hotta, Wild type, but not mutant-type, p53 enhances nuclear accumulation of the NS3 protein of hepatitis C virus, Biochem. Biophys. Res. Commun. 230 (1997) 431–436.

[23] S. Muramatsu, S. Ishido, T. Fujita, M. Itoh, H. Hotta, Nuclear localization of the NS3 protein of hepatitis C virus and factors affecting the localization, J. Virol. 71 (1997) 4954–4961.

[24] S. Ishido, H. Hotta, Complex formation of the nonstructural protein 3 of hepatitis C virus with the p53 tumor suppressor, FEBS Lett. 438 (1998) 258–262.

[25] S. Ogata, R.H. Florese, M. Nagano-Fujii, R. Hidajat, L. Deng, Y. Ku, S. Yoon, T. Saito, S. Kawata, H. Hotta, Identification of hepatitis C virus (HCV) subtype 1b strains that are highly, or only weakly, associated with hepatocellular carcinoma on the basis of the secondary structure of an amino-terminal portion of the HCV NS3 protein, J. Clin. Microbiol. 41 (2003) 2835–2841.

[26] T. Takehara, N. Hayashi, Y. Miyamoto, M. Yamamoto, E. Mita, H. Fusamoto, T. Kamada, Expression of the hepatitis C virus genome in

rat liver after cationic liposome-mediated in vivo gene transfer, Hepatology 21 (1994) 746–751.
[27] T. Tamura, N. Aoyama, H. Saya, H. Haga, S. Futami, M. Miyamoto, T. Koh, T. Ariyasu, M. Tachi, M. Kasuga, R. Takahashi, Induction of Fas-mediated apoptosis in p53-transfected human colon carcinoma cells, Oncogene 11 (1995) 1939–1946.
[28] R.H. Florese, M. Nagano-Fujii, Y. Iwanaga, R. Hidajat, H. Hotta, Inhibition of protein synthesis by the nonstructural proteins NS4A and NS4B of hepatitis C virus, Virus Res. 90 (2002) 119–131.
[29] K. Machida, K.T.-N. Cheng, V.M.-H. Sung, S. Shimodaira, K.L. Lindsay, A.M. Levine, M.-Y. Lai, M.M.C. Lai, Hepatitis C virus induces a mutator phenotype: enhanced mutations of immunoglobulin and protooncogenes, Proc. Natl. Acad. Sci. USA 101 (2004) 4262–4267.
[30] K. Machida, K.T.-H. Cheng, V.M.-H. Sung, K.J. Lee, A.M. Levine, M.M.C. Lai, Hepatitis C virus infection activates the immunologic (type II) isoform of nitric oxide synthase and thereby enhances DNA damage and mutations of cellular genes, J. Virol. 78 (2004) 8835–8843.
[31] R.A. Love, H.E. Parge, J.A. Wickersham, Z. Hostomsky, N. Habuka, E.W. Moomaw, T. Adachi, Z. Hostomska, The crystal structure of hepatitis C virus NS3 proteinase reveals a trypsin-like fold and a structural zinc binding site, Cell 87 (1996) 331–342.
[32] J.L. Kim, K.A. Morgenstern, C. Lin, T. Fox, M.D. Dwyer, J.A. Landro, S.P. Chambers, W. Markland, C.A. Lepre, E.T. O'Malley, S.L. Harbeson, C.M. Rice, M.A. Murcko, P.R. Caron, J.A. Thomson, Crystal structure of the hepatitis C virus NS3 protease domain complexed with a synthetic NS4A cofactor peptide, Cell 87 (1996) 343–355.

Journal of General Virology (2005), 86, 2197–2208 DOI 10.1099/vir.0.80862-0

Hepatitis C virus NS3 protein interacts with ELKS-δ and ELKS-α, members of a novel protein family involved in intracellular transport and secretory pathways

Rachmat Hidajat,[1] Motoko Nagano-Fujii,[1] Lin Deng,[1] Motofumi Tanaka,[1,2] Yuki Takigawa,[1] Sohei Kitazawa[3] and Hak Hotta[1]

Divisions of Microbiology[1], Gastroenterological Surgery[2] and Molecular Pathology[3], Kobe University Graduate School of Medicine, 7-5-1 Kusunoki-cho, Chuo-ku, Kobe 650-0017, Japan

Correspondence
Hak Hotta
hotta@kobe-u.ac.jp

The NS3 protein of hepatitis C virus (HCV) has a serine protease activity in its N-terminal region, which plays a crucial role in virus replication. This region has also been reported to interact not only with its viral cofactor NS4A, but also with a number of host-cell proteins, which suggests a multifunctional feature of NS3. By means of yeast two-hybrid screening using an N-terminal region of NS3 as bait, a human cDNA encoding a region of ELKS-δ, a member of a novel family of proteins involved in intracellular transport and secretory pathways, was molecularly cloned. Using co-immunoprecipitation, GST pull-down and confocal and immunoelectron microscopic analyses, it was shown that full-length NS3 interacted physically with full-length ELKS-δ and its splice variant, ELKS-α, both in the absence and presence of NS4A, in cultured human cells, including Huh-7 cells harbouring an HCV subgenomic RNA replicon. The degree of binding to ELKS-δ varied with different sequences of the N-terminal 180 residues of NS3. Interestingly, NS3, either full-length or N-terminal fragments, enhanced secretion of secreted alkaline phosphatase (SEAP) from the cells, and the increase in SEAP secretion correlated well with the degree of binding between NS3 and ELKS-δ. Taken together, these results suggest the possibility that NS3 plays a role in modulating host-cell functions such as intracellular transport and secretion through its binding to ELKS-δ and ELKS-α, which may facilitate the virus life cycle and/or mediate the pathogenesis of HCV.

Received 27 December 2004
Accepted 11 April 2005

INTRODUCTION

Hepatitis C virus (HCV) is the causative agent of non-A, non-B hepatitis (Choo *et al.*, 1989). It has been estimated that more than 170 million individuals are infected with HCV worldwide, representing nearly 3 % of the world's population (WHO, 1999). The majority of patients remain chronically infected, suffering from chronic liver disorders such as chronic hepatitis, liver cirrhosis and hepatocellular carcinoma (HCC).

HCV, an enveloped RNA virus, belongs to the genus *Hepacivirus* of the family *Flaviviridae*. The HCV genome is a single-stranded, positive-sense RNA of approximately 9·6 kb, which contains a large open reading frame (ORF) flanked by 5′- and 3′-untranslated regions (Reed & Rice, 2000). The ORF encodes a polyprotein of approximately 3000 aa, which is cleaved by the cellular signal peptidase and two virally encoded proteases into at least 10 mature proteins: core, envelope glycoprotein 1 (E1), E2, p7, non-structural protein 2 (NS2), NS3, NS4A, NS4B, NS5A and NS5B (Hijikata *et al.*, 1991, 1993).

NS3 is comprised of two domains, one possessing a serine protease activity and the other an RNA helicase activity, both of which are essential for virus replication. The protease domain resides in the N-terminal part of NS3, while the helicase domain is in the C-terminal part. NS3 enzymic activities are modulated by NS4A, which forms a complex with NS3 to stabilize and localize it to the perinuclear endoplasmic reticulum (ER) membranes (Reed & Rice, 2000; Wölk *et al.*, 2000). NS3 also interacts with the other NS proteins, either directly or indirectly through host-cell proteins, to form the virus replication complex (Aizaki *et al.*, 2004).

The interactions between NS3 and cellular proteins have been studied to elucidate its role(s) in viral pathogenesis (Reed & Rice, 2000; Tellinghuisen & Rice, 2002). The helicase domain of NS3 was shown to interact with protein kinase A (Aoubala *et al.*, 2001; Borowski *et al.*, 1999a). It was

The primer sequences used in this study are available as supplementary material in JGV Online.

also reported that NS3 served as a substrate for protein kinase C (PKC) and inhibited PKC signalling via competition with its physiological substrates (Borowski *et al.*, 1999b). NS3 also binds to histones H2B and H4 (Borowski *et al.*, 1999c). The NS3 helicase domain has also been shown to be essential for NS3 protein methylation by the protein arginine methyltransferase 1 (Rho *et al.*, 2001).

Studies on the NS3 serine protease domain have demonstrated that it can transform NIH3T3 cells (Sakamuro *et al.*, 1995), rat fibroblasts (Zemel *et al.*, 2001) and the human liver cell line QSG7701 (He *et al.*, 2003), although the underlying mechanism(s) remains to be elucidated. Previously, we reported that the oncogenic properties of NS3 might involve an interaction with the tumour suppressor p53 (Ishido & Hotta, 1998; Muramatsu *et al.*, 1997). The protease domain of NS3 has also been reported to bind to Sm-D1, a component of small nuclear ribonucleoprotein associated with autoimmune disease (Iwai *et al.*, 2003). A more recent study demonstrated that the protease domain of NS3 interacts with LMP7, a component of the immunoproteasome, and downregulated the proteasome peptidase activity (Khu *et al.*, 2004).

To identify another possible cellular target(s) that interacts with the NS3 protease domain, we screened a human cDNA library using a yeast two-hybrid system. We have shown here that NS3, through its protease domain, binds to ELKS-δ and its splice variant, ELKS-α (Nakata *et al.*, 1999, 2002). Since a mouse homologue of ELKS-δ, namely Rab6-interacting protein 2B (Rab6IP2B), was reported to affect intracellular transport by binding to Rab6 (Monier *et al.*, 2002), we tested the possible effects of NS3–ELKS-δ interaction on intracellular transport and secretory pathways using a secreted alkaline phosphatase (SEAP) assay. We observed that NS3 augmented the cellular secretion of SEAP and that the increase in SEAP secretion was proportional to the degree of binding between NS3 and ELKS-δ. These results collectively suggest the possibility that NS3 affects intracellular transport and/or secretion pathways by interacting with ELKS-δ and ELKS-α.

METHODS

Plasmid construction. cDNA fragments encoding an N-terminal portion of NS3 (aa 1027–1208) were amplified from sera of HCV-1b-infected patients by RT-PCR as described previously (Ogata *et al.*, 2002, 2003), with minor modifications, using the primers NS3-F and NS3-181R (see Supplementary Table in JGV Online). The amplified fragments were subcloned in frame to the LexA DNA-binding domain of pHybLex/Zeo (Invitrogen) to generate pLex-NS3-H-31 and pLex-NS3-H-45 for expression in yeast. Frame-shift mutants of bait (pLex-NS3-H-31-FS) and prey [pB42-ELKS-δ(787–1063)-FS] were generated by digesting the parental plasmids with *Eco*RI and *Bam*HI, respectively, followed by blunt-end formation and self-ligation. They served as negative controls. pB42-ATF6-α (Tong *et al.*, 2002) was also used as a negative control in this study.

A mammalian expression plasmid encoding Myc-tagged full-length NS3 [pcDNA3.1/NS3F(MKC1a)] was constructed by amplifying a cDNA fragment from pBSNS3/1027–1657 (Muramatsu *et al.*, 1997) using primers NS3/M/B and NS3F*Hin*dIII (Supplementary Table), followed by subcloning into pcDNA3.1/*myc*-His(−)C (Invitrogen). Expression plasmids for chimeric forms of full-length NS3 were constructed, in which the N-terminal 180 residues were derived from clinical isolates, nos 42, 45, H05-5 and H17-2 (Ogata *et al.*, 2002, 2003; GenBank accession nos AB072084, AB072086, AB072048 and AB072055, respectively), while the C-terminal 451 residues were derived from MKC1a (GenBank accession no. D45172). These plasmids were designated pcDNA3.1/NS3(M-42), pcDNA3.1/NS3-(M-45) pcDNA3.1/NS3(M-H05-5) and pcDNA3.1/NS3(M-H17-2), respectively.

A GST fusion protein-expressing plasmid was also constructed. A vector plasmid, pcDNA3.1/GST, was constructed by introducing a 767 bp *Hin*cII fragment of pGEX-4T1 (Pharmacia) into *Eco*RI-digested, blunt-ended pcDNA3.1/*myc*-His(−)C. The full-length NS3-coding region of MKC1a was subcloned in frame to pcDNA3.1/GST to generate pcDNA3.1/GST-NS3. pBS-GST-NS4B-F (Tong *et al.*, 2002) and pBS-GST-NS5A-F (Taguchi *et al.*, 2004) served as negative controls in this study.

Expression plasmids for FLAG-tagged, full-length ELKS-δ and ELKS-α were constructed. cDNA fragments of 3889 and 3834 bp encoding N-terminally deleted ELKS-δ and ELKS-α, respectively, were obtained by digesting pDR2-ELKS-δ and pDR2-ELKS-α (kind gifts from Dr M. Emi, Institute of Gerontology, Nippon Medical School, Kawasaki, Kanagawa, Japan) with *Bam*HI and *Xba*I and subcloned into the pcDNA3.1/N-FLAG vector (Tong *et al.*, 2002). Subsequently, a 718 bp sequence of ELKS-δ or ELKS-α (from the ATG initiation codon to the *Bam*HI site) was amplified by PCR from pDR2-ELKS-δ or pDR2-ELKS-α using the primers ELKS-F and ELKS-303R (Supplementary Table) and subcloned into the above plasmids. The resultant plasmids were designated pcDNA3.1/N-FLAG-ELKS-δ and pcDNA3.1/N-FLAG-ELKS-α. In addition, various deletion mutants of ELKS-δ were constructed by PCR using appropriate sets of primers (Supplementary Table), followed by subcloning into the expression vector.

Yeast two-hybrid screening. Yeast two-hybrid screening was performed using a Hybrid Hunter kit (Invitrogen) and a human cDNA library, as reported previously with some modifications (Tong *et al.*, 2002). In brief, the L40 yeast strain carrying pLex-NS3-H31 was transformed with the pYESTrp cDNA library prepared from HeLa cells (Invitrogen). Transformants were screened for growth on YC-WHUKZ300 plates lacking tryptophan, histidine, uracil and lysine but containing Zeocin. The resultant colonies were tested for β-galactosidase (β-Gal) activity according to the manufacturer's protocol.

Cell culture and protein expression. Vaccinia virus T7 hybrid expression was performed as reported previously (Muramatsu *et al.*, 1997). In brief, HeLa cells were inoculated with recombinant vaccinia virus expressing T7 RNA polymerase (vTF7-3). After virus adsorption for 1 h, cells were transfected with expression plasmids using Lipofectin (Invitrogen) and incubated overnight. Cells were then analysed for possible protein–protein interactions (see below). For immunofluorescence and the SEAP secretion assay, a plasmid-based expression method was employed using Fugene 6 transfection reagent (Roche). Cells were then incubated for 48 h before analysis.

A Huh-7 cell line stably harbouring an HCV subgenomic RNA replicon was prepared as described previously (Lohmann *et al.*, 2001; Taguchi *et al.*, 2004; Takigawa *et al.*, 2004), using pFK2884Gly (a kind gift from Dr R. Bartenschlager, University of Heidelberg, Heidelberg, Germany). A cured Huh-7 cell line was prepared by maintaining the stable HCV replicon-harbouring cell line in the presence of α-interferon (1000 IU ml^{-1}) for 1 month.

Double-staining immunofluorescence. Cells expressing Myc-tagged NS3 and FLAG-tagged ELKS-δ were fixed with 4 % paraformaldehyde at room temperature for 15 min and permeabilized with 100 % methanol at −20 °C for 3 min. Cells were then blocked with 5 % normal donkey serum for 1 h at room temperature. Primary antibodies used were anti-Myc mouse monoclonal antibody (Santa Cruz Biotech) and anti-FLAG rabbit polyclonal antibody (Sigma). FITC-conjugated goat anti-mouse IgG (MBL) and Cy3-conjugated donkey anti-rabbit IgG (Chemicon) were used as secondary antibodies, respectively. Stained cells were observed with a laser-scanning confocal microscope (LSM510 version 3.0; Carl Zeiss) or a fluorescence microscope (BX51; Olympus) attached to a DP70 CCD camera.

Immunoelectron microscopy. Cells expressing Myc-tagged NS3 and FLAG-tagged ELKS-δ were fixed with 4 % paraformaldehyde and 0·2 % glutaraldehyde for 30 min at room temperature. After washing with PBS, cells were centrifuged at 1500 r.p.m. for 5 min. The cell pellet was dehydrated in a series of 70, 80 and 90 % ethanol, embedded in LR White resin (London Resin) and kept at −20 °C for 2 days to facilitate resin polymerization. After ultrathin sectioning, samples were etched in 3 % H_2O_2 for 5 min at room temperature and washed with PBS. For labelling, sections were incubated with anti-Myc mouse monoclonal antibody and anti-FLAG rabbit antiserum for 1 h. After rinsing with PBS, sections were incubated with goat anti-mouse IgG and goat anti-rabbit IgG conjugated to 5 and 10 nm gold particles (Sigma), respectively, for 1 h. Sections were post-stained with uranyl acetate and lead citrate and observed under a transmission electron microscope (JEM 1200EX; JEOL).

Co-immunoprecipitation. Cells expressing Myc-tagged NS3 and FLAG-tagged ELKS-δ or ELKS-α were lysed in ice-cold RIPA buffer (1 × PBS, 1 % NP-40, 0·5 % sodium deoxycholate, 0·1 % SDS) with freshly added protease inhibitors (PMSF and aprotinin). Lysates were centrifuged at 10 000 *g* for 10 min at 4 °C and the supernatants were mixed with 0·25 μg normal rabbit IgG and 20 μl protein G–agarose beads (Pharmacia) at 4 °C for 30 min to eliminate non-specific binding. The pre-cleared lysates were incubated with anti-Myc rabbit polyclonal antibody for 1 h at 4 °C, followed by incubation with 20 μl protein G–agarose beads for another 1 h. After five washes with ice-cold RIPA buffer, the immunoprecipitates were analysed by immunoblotting, as described below.

Immunoblotting. Samples were subjected to SDS-PAGE and blotted electrophoretically on to a PVDF membrane (Immobilon-P; Millipore). After blocking in PBS containing 5 % skimmed milk, membranes were incubated with anti-FLAG or anti-Myc mouse monoclonal antibody for 1 h. Membranes were then incubated with peroxidase-labelled goat anti-mouse IgG (MBL) for 1 h. After three washes, protein bands were visualized by enhanced chemiluminescence (Amersham Biosciences). Densitometric analysis was performed using publicly available software (tnimage-3.3.14; available at http://brneurosci.org/tnimage.html).

GST pull-down assay. Lysates were prepared from cells transiently expressing GST-tagged NS3 and FLAG-tagged ELKS-δ or ELKS-α. Lysates were mixed with 20 μl glutathione-conjugated Sepharose 4B beads at 4 °C for 90 min. The beads were washed five times with ice-cold RIPA buffer and subjected to immunoblot analysis using anti-FLAG antibody. To verify that there was a comparable amount of protein in each sample, lysates were directly (without pull-down) subjected to immunoblotting.

SEAP secretion assay. A SEAP secretion assay was performed to measure the possible effect of NS3 on the secretory pathway. SEAP is a genetically engineered secreted form of alkaline phosphatase (Cullen & Malim, 1992) and the SEAP secretion assay has been widely used to monitor cellular secretory function including Rab6-mediated intracellular transport (Echard *et al.*, 2000; Martinez *et al.*, 1994). HeLa cells were transiently transfected with 200 ng pcDNA3.1-derived NS3 expression plasmid, 50 ng pSEAP2-Control (BD Biosciences) and 1 ng pRL-SV40 (Promega), in the presence or absence of 200 ng pcDNA3.1/N-Flag-ELKS-δ. pRL-SV40 was used to express *Renilla* luciferase as an internal control. After 48 h, culture medium was collected for the SEAP secretion assay, while the cells were processed for the *Renilla* luciferase assay. SEAP activity was measured using the SEAP Reporter Gene Assay (Roche) and *Renilla* luciferase activity measured using the *Renilla* Luciferase Assay System (Promega), according to the manufacturers' instructions. SEAP activity in each sample was normalized against *Renilla* luciferase activity. Since pSEAP2-Control and pRL-SV40 use the same SV40 early promoter, the marginal effect of NS3 on promoter activity (an increase of ~20 %, as determined by *Renilla* luciferase activity) was nullified and the effect on SEAP secretion could be determined by this assay.

RESULTS

Identification of ELKS-δ as an NS3-interacting protein using a yeast two-hybrid assay

To identify a human protein(s) that physically interacts with the NS3 protease domain (aa 1027–1208) (Fig. 1a), the L40 yeast strain harbouring pLex-NS3-H-31 was transformed with the pYESTrp-based HeLa cDNA library and screened for growth on YC-WHUKZ300 selection plates. Out of $5{\cdot}8 \times 10^7$ primary transformants screened, 260 colonies grew on the selection plates. Further screening for β-Gal activity identified a clone that showed strong reactivity. DNA sequence analysis revealed that the yeast clone carried a pYESTrp-driven sequence that completely matched the sequence for a C-terminal portion of ELKS-δ (GenBank accession no. AB053470; Nakata *et al.*, 2002). The cloned cDNA fragment was designated ELKS-δ(787–1063).

The specificity of the interaction between NS3 and ELKS-δ(787–1063) was tested by transfecting the parental (naïve) L40 strain with various combinations of expression plasmids, including two different NS3 sequences (H-31 and H-45) and frame-shift mutants of NS3-H-31 and ELKS-δ(787–1063). The results demonstrated specific interaction between the NS3 protease domain and ELKS-δ(787–1063) in yeast (Fig. 1b).

NS3 interacts with ELKS-δ and its splice variant, ELKS-α, in cultured human cells

The interaction between NS3 and ELKS-δ was further investigated in mammalian cells and a specific interaction between the protease domain of NS3 and ELKS-δ(787–1063) was observed (data not shown). Moreover, full-length NS3 (aa 1027–1657) was shown to interact with ELKS-δ(787–1063) in HeLa cells (Fig. 2a, lane 2). We then narrowed down the region of ELKS-δ responsible for the interaction with full-length NS3 (Fig. 2b). C-terminal truncation of ELKS-δ up to aa 1008 did not affect the interaction with NS3. However, further deletion up to aa 995 or 979 abolished the ability to interact with NS3. N-terminal truncation of the initial fragment up to aa 846 did

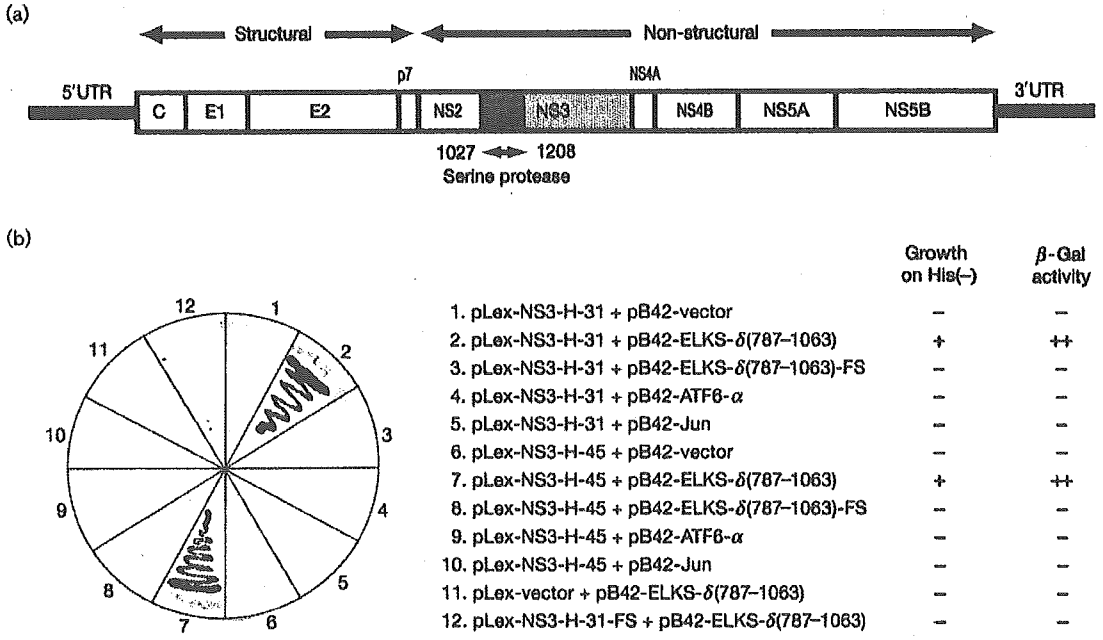

Fig. 1. Identification of ELKS-δ as an NS3-binding protein by yeast two-hybrid assay. (a) Schematic diagram of the HCV genome. The N-terminal serine protease domain of NS3 (aa 1027–1208) used as bait is also depicted. (b) A representative result showing specific interaction between the NS3 protease domain and ELKS-δ(787–1063). The L40 yeast strain co-transfected with the indicated plasmids was grown on tryptophan-deficient media containing the antibiotic Zeocin and subsequently assayed for β-Gal activity. Development of a blue colour within 30 min indicated strong interaction between the two proteins of interest. ++, Strong interaction; +, moderate interaction; –, no interaction.

not affect the interaction with NS3, while further deletion up to aa 876 or 886 completely abolished it. These results mapped a minimum NS3-interacting region somewhere between aa 846 and 1008 of ELKS-δ. ELKS-δ(846–1008) consistently interacted with NS3. Similar results were obtained using a yeast two-hybrid system (data not shown).

Next, we tested the interaction of full-length NS3 with full-length ELKS-δ and its splice variant, ELKS-α. GST pull-down analysis demonstrated that full-length NS3 interacted with full-length ELKS-δ and ELKS-α (Fig. 3a). The specificity of the interaction between NS3 and ELKS-δ was confirmed by demonstrating that neither NS4B nor NS5A of HCV bound to full-length ELKS-δ under the same experimental conditions (Fig. 3b). Specific interaction between the two molecules was also confirmed by co-immunoprecipitation analysis, in which anti-FLAG antibody (directed against FLAG-tagged full-length ELKS-δ and ELKS-α) co-immunoprecipitated full-length NS3 (data not shown).

In order to determine whether NS3 interacted with ELKS proteins in the presence of the other HCV non-structural proteins, we expressed ELKS-δ and ELKS-α in Huh-7 cells harbouring an HCV subgenomic RNA replicon and subsequently immunoprecipitated NS3 using anti-NS3 polyclonal antibody. The result demonstrated that NS3 expressed in the context of HCV replication interacted with full-length ELKS-δ and ELKS-α in HCV RNA replicon-harbouring cells (Fig. 3c).

Sequence comparison of ELKS-δ and ELKS-α

The amino acid sequences of ELKS-δ and ELKS-α differ from each other in their C-termini due to alternative splicing (Fig. 4a). As described above, a minimum region responsible for the interaction with NS3 was mapped between aa 846 and 1008 of ELKS-δ (Fig. 2). Since full-length ELKS-α interacted with NS3 (Fig. 3), we then determined a minimum region of ELKS-α responsible for the interaction. Deletion mutational analysis revealed that ELKS-α(747–948), but not ELKS-α(763–948), ELKS-α(791–948) or ELKS-α(806–948), interacted with NS3 (Fig. 4b and c), suggesting that ELKS-α(747–948) is the minimum region responsible for the interaction with NS3.

NS3 co-localizes with ELKS-δ in human cells

We visualized the co-localization of NS3 with ELKS-δ in Huh-7 cells by double-staining immunofluorescence

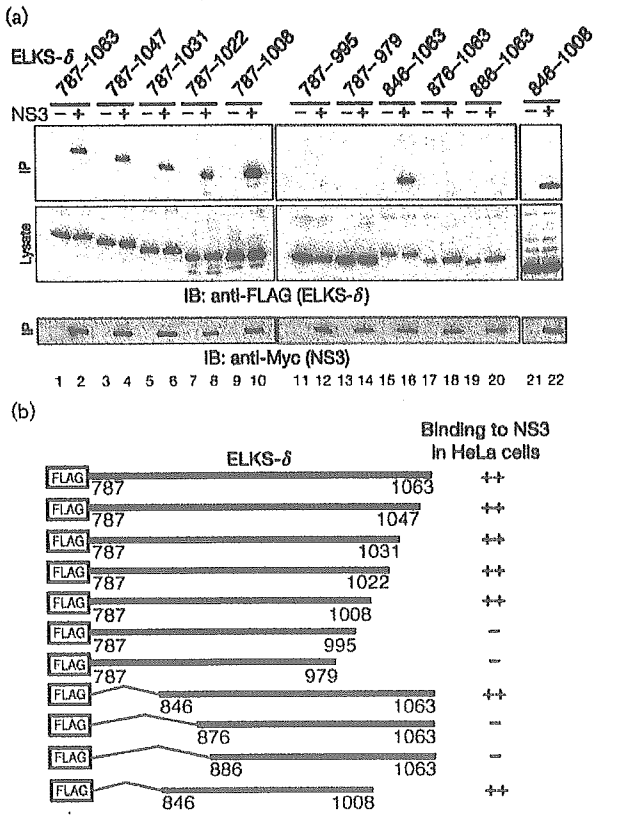

Fig. 2. Determination of the minimum region of ELKS-δ required for interaction with full-length NS3 in cultured human cells. (a) A series of deletion mutants of FLAG-tagged ELKS-δ was expressed by the vaccinia–T7 hybrid expression method in HeLa cells without (odd-numbered lanes) or with (even-numbered lanes) Myc-tagged full-length NS3. Cell lysates were immunoprecipitated using anti-Myc antibody and probed by immunoblotting using anti-FLAG antibody (upper panel). Lysates were directly (without being immunoprecipitated with anti-Myc antibody) probed with anti-FLAG antibody to verify a comparable degree of expression of the ELKS-δ mutants (middle panel). Efficient immunoprecipitation of Myc-tagged NS3 with anti-Myc antibody was also verified (lower panel). (b) Schematic diagram of the various deletion mutants of ELKS-δ. ++, Strong interaction; −, no interaction.

analysis. When co-expressed in Huh-7 cells using plasmid-based expression methods, full-length NS3 co-localized with full-length ELKS-δ in the cytoplasm, both in the absence (Fig. 5a) and presence (Fig. 5b) of NS4A. Co-localization of NS3 with ELKS-δ was also observed in HCV RNA replicon-harbouring cells (Fig. 5c).

Immunoelectron microscopic analysis also demonstrated co-localization of full-length NS3 with full-length ELKS-δ in close proximity to the ER membranes in the perinuclear region (Fig. 5d).

NS3 interacts differentially with ELKS-δ in an NS3 sequence-dependent manner

A considerable degree of sequence variation has been observed in the N-terminal 180 residues of NS3 (Ogata *et al.*, 2002, 2003). We performed experiments to determine whether or not interaction with ELKS-δ varied with different NS3 sequences. We first used 198-residue fragments of NS3 obtained from four patients (nos 42, 45, H05-5 and H17-2) and found that the degree of interaction with ELKS-δ varied with the different sequences (data not shown). Next, we tested full-length NS3 sequences of five different isolates, a parental strain (MKC1a) and four chimeric forms (M-42, M-45, M-H05-5 and M-H17-2), which differed from each other by at most 10 residues within the N-terminal 180 residues, all having the remaining C-terminal 451 residues in common. These full-length forms of NS3 were each expressed with full-length ELKS-δ and the interactions examined. Consistent with the results obtained with the 198-residue fragments, the degree of interaction between full-length NS3 and ELKS-δ varied with the different NS3 sequences, with M-42 and M-45 showing the strongest interaction, and M-H05-5 the weakest (Fig. 6a and b). Sequence alignment of the N-terminal 180 residues of NS3 is shown in Fig. 6(c). Five residues (Val-1044, Leu-1106, Ala-1176, Val-1179 and Ile-1196) were unique to M-H05-5. Based on this sequence alignment alone, however, it was difficult to draw a conclusion as to which residue(s) most significantly affects the interaction with ELKS-δ.

When NS4A was co-expressed, the interaction between NS3 and ELKS-δ became weaker, although still detectable, and the NS3 sequence-dependent difference in the interaction with ELKS-δ was not clearly observed (data not shown).

NS3 enhances SEAP secretion from the cell, possibly through its interaction with ELKS-δ

The binding domain of Rab6IP2, a murine homologue of ELKS-δ, has been reported to affect the endosome-to-Golgi retrograde transport pathway through its binding to Rab6 (Monier *et al.*, 2002). CAST and ERC proteins, rat homologues of the ELKS protein family, have also been implicated in the modulation of neurotransmitter secretion (Deguchi-Tawarada *et al.*, 2004; Ohtsuka *et al.*, 2002; Wang *et al.*, 2002). We thought that NS3 might affect the possible function of ELKS-δ and/or its splice variant(s), modulating intracellular transport and secretory function. Therefore, we performed a SEAP assay. The results demonstrated that SEAP secretion was significantly enhanced by NS3 of three isolates (MKC1a, M-42 and M-45), especially when ELKS-δ was expressed ectopically (Fig. 7a). In this context, we assumed that endogenous ELKS-δ was also expressed, although to a lesser extent. In contrast, NS3 of the other isolates (M-H-05-5 and M-H17-2) did not enhance SEAP secretion in the absence of ectopic ELKS-δ, while a mild enhancement by NS3 of M-H17-2 was